SEMMELWEIS EGYETEM

DOKTORI ISKOLA

Ph.D. értekezések

2892.

ALEX ALI SAYOUR

Szív- és érrendszeri betegségek élettana és klinikuma
című program

Programvezető: Dr. Merkely Béla, egyetemi tanár

Témavezető: Dr. Radovits Tamás, egyetemi tanár

CHARACTERIZATION OF MYOCARDIAL SODIUM–GLUCOSE COTRANSPORTER 1 EXPRESSION IN HEART FAILURE

PhD thesis

Alex Ali SAYOUR, M.D.

Doctoral School of Theoretical and Translational Medicine

Semmelweis University

Supervisor: Tamás Radovits, M.D., Ph.D.

Official reviewers: Tamás Habon, M.D., Ph.D.
Attila Fintha, M.D., Ph.D.

Head of the Complex Examination Committee:

István Karádi, M.D., D.Sc.

Members of the Complex Examination Committee:

Henriette Farkas, M.D., D.Sc.
Hassan Charaf, D.Sc.

Budapest

2023

Table of Contents

List of abbreviations

3–NT: 3–nitrotyrosin

4–HNE: 4–hydroxy–2–nonenal

α– or β–MHC: α– or β–myosin heavy chain

ACC: acetyl coenzyme–A carboxylase

ACF: aortocaval fistula

AMPKα: adenosine–monophosphate–activated protein kinase catalytic α subunit

ANCOVA: analysis of covariance

ANOVA: analysis of variance

a.u.: arbitrary units

AWT: anterior wall thickness

Col1a1: collagen type I alpha 1

CRT: cardiac resynchronization therapy

CTGF: connective tissue growth factor

DAPI: 4',6–diamidino–2–phenylindole

DCM: dilated cardiomyopathy

EF: ejection fraction

ERK1/2: extracellular signal–regulated kinase 1/2 (p44/42 mitogen–activated protein kinase, MAPK)

ESPVR: end–systolic pressure–volume relationship

f.c.: fold change

GAPDH: glyceraldehyde–3–phosphate dehydrogenase

GLUT1 or GLUT4: glucose transporter type 1 or 4

HCM: hypertrophic cardiomyopathy

HF: heart failure

IHD: ischemic heart disease

LV: left ventricle or left ventricular

LVEDD: left ventricular end–diastolic diameter

LVESP: left ventricular end–systolic pressure

Na–K–ATPase: sodium–potassium ATPase

NADPH: nicotinamide adenine dinucleotide phosphate

NCX: Na^+/Ca^{2+} exchanger

NHE1 = Na^+/H^+–exchanger

Nox4: nicotinamide adenine dinucleotide phosphate oxidase 4

PV: pressure–volume

PWT: posterior wall thickness

RIN: RNA integrity number

ROS: reactive oxygen species

r_s: Spearman's rho

SEM: standard error of the mean

SGLT1 or SGLT2: sodium–glucose cotransporter 1 or 2

SLC5A1 or SLC5A2: solute carrier family 5 member 1 or 2

T2DM: type 2 diabetes mellitus

TAC: transverse aortic constriction

Tau: time constant of left ventricular pressure decay

TBST: Tris–buffered saline Tween 20

TGF–β: transforming growth factor–β

1. Introduction

Heart failure (HF) is a clinical syndrome with characteristic symptoms and signs related to structural or functional cardiac anomaly (1). The diagnosis of HF is supported by increased levels of markers of congestion (natriuretic peptides) or objective evidence of pulmonary or systemic congestion (1). In the clinical setting, left–sided HF is classified based on left ventricular (LV) systolic function, namely, ejection fraction (EF). Accordingly, three EF categories are defined: HF with reduced (EF≤40%), mildly reduced (EF 41–49%), and preserved (EF≥50%) LV EF (1). Recently, HF has been described as a 'pandemic', affecting more than 64 million people worldwide as of 2017 (2), its prevalence (currently 1–3% in the general adult population) is expected to continuously increase in the coming years (3). Importantly, diagnosing an average adult patient with HF translates into up to 15–30% risk of death within one year of the diagnosis, and up to 50–75% risk of death within the forthcoming five years depending on the severity of HF, despite medical therapy (3). This means that the prognosis of HF is much worse than that of a number of malignant diseases. On top of this, HF is associated with substantial morbidity and significant impairment of functional capacity and quality of life, ultimately resulting in extremely high healthcare costs (3). These necessitate the need for intensive research on the prevention of HF, and on treatment options designed to treat manifest HF.

Type 2 diabetes mellitus (T2DM), a condition characterized by increased blood sugar levels due to relative lack of insulin, is another 'pandemic' with steadily increasing incidence (4). Importantly, T2DM constitutes an increased risk for HF, vice versa, T2DM is more prevalent in patients with HF, possibly due to the intertwined pathophysiological background of the two conditions (5). Based on these, one might speculate that T2DM and HF could be targeted with the same medications. However, concern emerged about the cardiovascular safety of some antidiabetic agents. Specifically, a highly influential meta–analysis (6) showed that the antidiabetic agent rosiglitazone (member of the thiazolidinedione class) increases the risk of myocardial infarction and cardiovascular mortality in patients with T2DM. Accordingly, in 2008, the Food and Drug Administration of the United States of America forced pharmaceutical manufacturers to conduct cardiovascular outcome trials with newly marketed antihyperglycemic agents to prove safety (7). Therefore, the novel class of

antihyperglycemic agents, sodium–glucose cotransporter 2 (SGLT2) inhibitors, had to be tested in such studies. In accordance, several large cardiovascular outcome trials in high–risk T2DM patients have been conducted with selective SGLT2 inhibitors and a dual SGLT1/2 inhibitor (8-13). Not only these medications have proven to be safe in these patients with T2DM, but they have shown robust salutary cardiorenal protection as a class effect. Specifically, all these agents reduced the risk of hospitalization for HF without significant heterogeneity (14). Later it was found that this effect is independent of the presence of T2DM, yet, the exact mechanism of action is currently incompletely understood (15).

In the next sections, the importance of SGLT2 inhibitors in HF is discussed in clinical and mechanistic contexts.

1.1. The rationale behind pharmacological SGLT2 and SGLT1 inhibition

The pharmacological antidiabetic action of SGLT2 inhibitors is based on the blockade of SGLT2 in the kidney, a high–capacity low–affinity glucose transporter that uses one sodium ion per glucose molecule to transport glucose into the intracellular space (16). It is located in the brush border of the proximal convoluted tubule (S1/S2 segment) of kidney nephrons accounting for the reabsorption of the majority of glucose (~97%) under normoglycemic conditions (17). On the contrary, the low–capacity high–affinity SGLT1, which shows structural similarity to SGLT2 and transports two sodium ions per glucose molecule into the intracellular space (18), is abundant in the brush border of the distal part (S3 segment) of the proximal convoluted tubule, and accounts for the reabsorption of remnant glucose (~3%) (19).

Since SGLT2 is upregulated in kidneys of humans (and rodents) with diabetes (20) and at the same time accounts for virtually all of glucose reabsorption in the kidney under baseline conditions, it is well–established that pharmacological inhibition of renal SGLT2 results in glucosuria, reducing serum glucose levels. However, selective SGLT2 inhibition is still associated with 40–50% glucose reabsorption, as it unleashes the transport capacity of the distal SGLT1 (19, 21), which compensates for the loss of SGLT2 activity in the kidney to some extent. Interestingly, the dual SGLT1/2 inhibitor sotagliflozin has similar glucosuric effect to selective SGLT2 inhibitors (22) but it

additionally blocks intestinal SGLT1, where SGLT1 shows the highest expression in the body, accounting for the vast majority of dietary glucose absorption (23). Herein, intestinal SGLT1 inhibition results in delayed glucose uptake and release of glucagon–like peptide 1, reducing post–prandial serum glucose excursions, which might contribute to improved glycemic control (24).

1.2. Cardiorenal benefits of pharmacological SGLT2 and SGLT1/2 inhibition in patients with and without type 2 diabetes mellitus

In compliance with the above mentioned mandate from the Food and Drug Administration in 2008, large cardiovascular outcome trials enrolling high–risk T2DM patients have been carried out with the following SGLT2 inhibitors: empagliflozin (8), canagliflozin (9, 11), dapagliflozin (10), and ertugliflozin (12). Overall, SGLT2 inhibitors turned out to exert only mild antidiabetic action, although, somewhat unexpectedly, a slight but significant beneficial effect was seen on major adverse cardiovascular events (14). Most striking, however, was the fact that all trials reported a highly significant ~32% relative reduction in risk of hospitalization for heart failure (HF) with no heterogeneity (25). The SCORED trial (13) further reinforced these findings with the dual SGLT1/2 inhibitor sotagliflozin. Notably, in all these trials, the event curves of hospitalization for HF separated rapidly, with significant difference already at 1 month as compared with placebo. Nonetheless, these were not dedicated HF trials.

The first dedicated HF trial with the SGLT2 inhibitor dapagliflozin (DAPA–HF) (26) showed that treatment resulted in significantly reduced risk of first worsening HF event and death from cardiovascular causes in patients with reduced EF, irrespective of the presence of T2DM. A similar reduction in the composite endpoint was documented in another dedicated HF trial (EMPEROR–Reduced) (27) in patients with reduced EF, again independent of the presence of diabetes. Therefore, the salutary cardiovascular effects of selective SGLT2 inhibitors are not confined to diabetic conditions in patients with HF. The dual SGLT1/2 inhibitor sotagliflozin was also tested in a dedicated HF trial (SOLOIST–WHF) (28), however, it exclusively enrolled patients with T2DM and recent hospitalization for worsening HF. The primary endpoint (composite of cardiovascular death, hospitalizations and urgent visits for HF) was sharply reduced by

33% in the sotagliflozin arm, as compared with placebo (28). Furthermore, the SOLOIST–WHF was the first dedicated HF trial ever to document a significant subgroup effect regarding the reduction in the risk of the primary endpoint in patients with HF and preserved EF (28). This effect was later corroborated by two dedicated HF trials (EMPEROR–Preserved and DELIVER) enrolling patients with mildly–reduced or preserved EF (29, 30). Large randomized cardiovascular outcome trials in patients with HF carried out with SGLT2 inhibitors are presented in Table 1.

Based on the above trial results, SGLT2 inhibitors are no longer simply antihyperglycemic agents, but represent a new class of HF medications on the whole spectrum of EF, regardless of diabetes. Not surprisingly, the current European Society of Cardiology guidelines recommend using SGLT2 inhibitors as disease-modifying agents in patients with HF and reduced EF besides beta–blockers, angiotensin converting enzyme inhibitors or sacubitril/valsartan, and mineralocorticoid receptor antagonists (31). Furthermore, there is a good reason to believe that the SGLT2 inhibitors dapagliflozin and empagliflozin will be recommended in future guidelines in patients with mildly reduced or preserved EF given their clinical efficacy. If so, then virtually all patients with HF (regardless of EF) should be assessed for eligibility for SGLT2 inhibitor treatment, which translates into tens of millions of people with HF worldwide. Furthermore, SGLT2 inhibitors are also indicated in patients with T2DM, and in those with chronic kidney disease (14).

Unfortunately, the expansion of patient groups eligible for SGLT2 inhibitor treatment far outpaces studies explaining the mechanism of action of these agents, which is currently incompletely understood (15). The structurally similar glucose transporter – SGLT1 – is non–specifically blocked by these agents. Interestingly, myocardial SGLT1 has recently been identified as a major myocardial glucose transporter in patients with HF alongside the well–established glucose transporter 1 and 4 (GLUT1 and GLUT4) (32). Unlike GLUTs which are uniporters that transport glucose into cardiomyocytes along its gradient of concentration, SGLT1 transports glucose into cardiomyocytes with a high energy cost, as it relies on the sodium concentration gradient (32). In the next sections, proposed mechanisms of SGLT2 inhibitors are described with special focus on their non–specifically blocked target, SGLT1, which is highly abundant in the failing heart.

Table 1. Dedicated placebo-controlled, randomized cardiovascular outcome trials of SGLT2 inhibitors in patients with HF

CI: confidence interval; CV: cardiovascular; HF: heart failure; HFmrEF: heart failure with mildly reduced ejection fraction; HFpEF: heart failure with preserved ejection fraction; HFrEF: heart failure with reduced ejection fraction; HR: hazard ratio; SGLT2: sodium-glucose cotransporter 2; T2DM: type 2 diabetes mellitus

Trial name (Acronym)	Patient population (number of)	SGLT2 inhibitor (vs. placebo)	Primary outcome	HR (95% CI) for primary outcome
DAPA–HF	HFrEF ± T2DM (4744)	dapagliflozin	worsening HF or CV death	0.74 (0.65, 0.85)
EMPEROR–Reduced	HFrEF ± T2DM (3730)	empagliflozin	hospitalization for worsening HF or CV death	0.75 (0.65, 0.86)
SOLOIST–WHF	hospitalization for HF + T2DM (1222)	sotagliflozin	hospitalizations and urgent visits for HF, or CV death	0.67 (0.52, 0.85)
EMPEROR–Preserved	HFmrEF or HFpEF ± T2DM (5988)	empagliflozin	hospitalization for HF or CV death	0.79 (0.69, 0.90)
DELIVER	HFmrEF or HFpEF ± T2DM (6263)	dapagliflozin	worsening HF or CV death	0.82 (0.73, 0.92)

1.3. Proposed mechanisms of cardiovascular protective effects of SGLT2 inhibitors – why myocardial SGLT1 matters

The fast separation of event curves and a class effect on HF outcomes warrants further investigation pertinent to the mechanism of action of SGLT2 inhibitors. To date, several mechanisms have been proposed (7, 33-42), which are summarized in Figure 1. Currently, the exact mechanism is unclear, but there is good reason to believe in pleiotropic actions, which might differ in importance in certain patient groups. For example, antihyperglycemic actions might not play a key role in non–diabetic patients with HF, in whom SGLT2 inhibitors are equally effective (26, 27, 43). Second, osmotic and natriuretic effects might also be less dominant, since SGLT2 inhibitors have little effect on markers of volume overload in patients with HF (26, 27, 44). In fact, beneficial clinical outcomes are equivalent in HF patients irrespective of whether or not

they experienced recent manifestation of volume overload (45). Third, salutary renal actions of SGLT2 inhibitors on top of diuretic effects have also been proposed independent of diabetic state (39), however, the effect on renal endpoints show some heterogeneity across particular SGLT2 inhibitors, while the effect on HF outcomes is homogeneous. Therefore, one might speculate that there is a unifying mechanism of action in patients with HF, which is less affected by differences in patient characteristics.

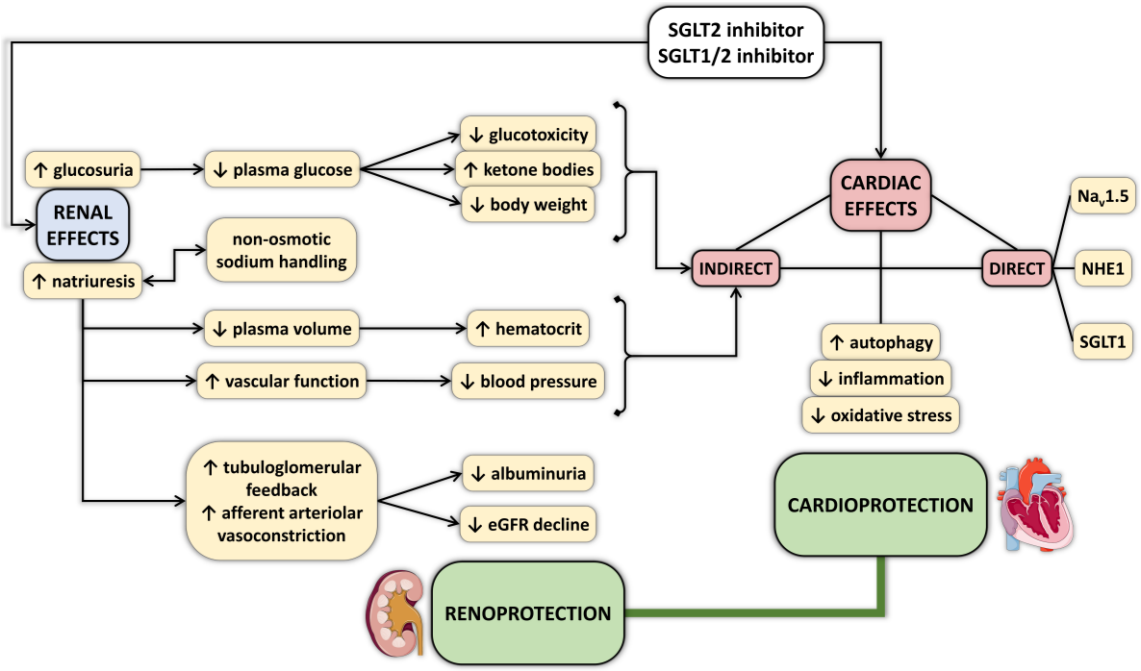

Figure 1. Summary of proposed mechanisms of salutary cardiorenal actions of SGLT2 and SGLT1/2 inhibitors.

eGFR: estimated glomerular filtration rate; NHE1 = Na^+/H^+–exchanger; SGLT1/2: sodium–glucose cotransporter 1/2

Indeed, there is a growing number of studies suggesting that SGLT2 inhibitors exert direct cardioprotective effects, though SGLT2 is not convincingly expressed in murine and human hearts (32, 46-49). Few studies have reported the possible membrane transporter in cardiomyocytes that might convey the signal of SGLT2 inhibitors into the intracellular space. The Na^+/H^+–exchanger 1 (NHE1) has recently been identified as a potential membrane transporter that is blocked by selective SGLT2 inhibitors in healthy rabbit, rat, and mouse cardiomyocytes (50-52). This effect seems to be vastly different

from that of the NHE1 inhibitor cariporide under pathological conditions (53), whereas others reported no substantial effect of SGLT2 inhibitors on NHE1 activity in cardiomyocytes (54). Finally, another study identified a sodium channel ($Na_v1.5$) in cardiomyocytes as a potential target for SGLT2 inhibitors (55), which needs further validation.

Interestingly, a recent study using docking analysis found that SGLT2 inhibitors show a relatively high binding affinity towards SGLT1, with much less affinity towards NHE1 (56). Given the wide range of the selectivity of SGLT2 inhibitors for SGLT2 over SGLT1 (ranging from ~20 to ~2700–fold (14, 57)), it is reasonable to speculate that less selective agents could bind to myocardial SGLT1 with higher potency, exerting direct cardiac actions. Importantly, SGLT1 is highly expressed in the myocardium (32, 46-49, 58) and its expression is altered in disease states (58).

An important way to appreciate relevance of a given transporter is by characterizing patients who lack the functional transporter due to genetic background. Loss–of–function mutations in the SLC5A1 gene encoding SGLT1 in humans is associated with so–called glucose/galactose malabsorption disorder, a rare autosomal recessive Mendelian disorder resulting in neonatal death if not corrected (59). This is because SGLT1 is the rate–limiting transporter in glucose and galactose absorption in the small intestine, complete loss–of–function results in severe diarrhea and dehydration (59). However, characterizing variants of the gene encoding SGLT1 resulting in only partial dysfunction of the transporter might demonstrate the systemic effects of pharmacological inhibition of SGLT1. In their study, Seidelmann and colleagues (60) performed whole exome sequencing in 5687 participants in the ARIC (Atherosclerosis Risk in Communities) registry. They reported that the frequency of missense mutations associated with reduced (but not completely lost) SGLT1 function is 6.7% (60). Patients with the identified haplotype had substantially lower risk of developing T2DM or HF (relative risk reduction in adjusted models: 29% and 26%, respectively) and reduced risk of death (relative risk reduction in adjusted model: 19%) as compared with unaffected controls (60). On the contrary, polymorphisms in the SLC5A2 gene (encoding SGLT2) are associated with small reductions in the incidence of HF or T2DM (both <3% relative risk reduction), whereas all–cause mortality is unaffected (61). Therefore, pharmacological blockade of SGLT1 might produce more pronounced

clinical benefits in HF as compared with SGLT2 inhibition only. These establish the potential pathophysiological relevance of SGLT1 inhibition in HF.

1.4. Changes in expression of SGLT1 in various myocardial disease states

Zhou and colleagues (46) showed that SGLT1 mRNA was present in human cardiomyocytes, its abundance was second only to that of the small intestine (46), the latter is a key target of the dual SGLT1/2 inhibitor sotagliflozin. Later it was found that capillaries of rat hearts (62) and human cardiac fibroblasts (63) also express SGLT1. Banerjee and colleagues (58) performed SGLT1 immunofluorescent staining on cardiomyocytes and speculated that it localized to the sarcolemma, which was corroborated in human and murine heart samples (49, 58, 64-66), as well as on the cardiomyocyte level (67, 68). However, Vrhovac and colleagues (69) found that SGLT1 did not co–localize with Na–K–ATPase in the human heart, instead it co–localized with aquaporin–1, a marker of capillaries. These authors postulated that SGLT1 expression in the heart is limited to the microvasculature (69). To resolve this dispute, data on high number of human HF samples are needed, which is currently missing.

Several studies documented that humans with HF exhibit increased LV SGLT1 mRNA or protein expression as compared with non–failing controls, including those with ischemic heart disease (IHD) (49, 58), hypertrophic cardiomyopathy (HCM) (49), and also those with HF and T2DM (58, 67), or mixed cohorts of these HF etiologies (67). Some studies found no significant difference in LV SGLT1 expression in patients with dilated cardiomyopathy (DCM) (32, 58), or IHD (32) compared with non–failing controls. To date, no comprehensive study has assessed the expression of LV SGLT1 on relatively large number of failing human heart samples with clinical context.

In line with data on human hearts, myocardial SGLT1 mRNA or protein expression was found to be upregulated in non–diabetic small animal models of acute myocardial ischemia–reperfusion injury (68) or ischemic preconditioning (65), permanent left anterior descending coronary artery ligation (model of IHD) (58, 64, 70), and chronic pressure overload–induced HF (71), as well as in models of metabolic syndrome and T2DM (58, 67, 72-75). Albeit some preclinical studies showed no significant alteration in myocardial SGLT1 expression in hearts of mice with metabolic syndrome (76), or

following permanent left anterior descending coronary artery ligation (77), or in models of acute ex vivo ischemia–reperfusion injury (76, 78). It is unclear whether SGLT1 is upregulated in HF regardless of the nature of hemodynamic overload.

Data are scarce regarding the mediators of SGLT1 upregulation in the heart, especially in HF. A previous study in humans showed increased activating phosphorylation of adenosine–monophosphate–activated protein kinase (AMPK) and extracellular signal–regulated kinase 1/2 (ERK1/2) in HF patients, in whom SGLT1 was upregulated (49). In a genetic small animal model of HF, overactivation of AMPK resulted in the development of HF with increased expression of LV SGLT1 (66, 79). Further studies are needed to elucidate how SGLT1 correlates with activation of these kinases in HF.

1.5. Pathophysiological role of myocardial SGLT1

Under basal conditions, neither global knock out (80, 81) nor cardiomyocyte–specific knock down (68) of SGLT1 alters baseline glucose uptake on the cardiomyocyte or myocardial level in murine hearts. Furthermore, no specific basal phenotype has been noted in these genetically–altered mice, as heart weight, myocardial structure and LV function are unchanged (48, 68, 79, 81).

On the cardiomyocyte level, there is evidence that SGLT1 facilitates increased ROS production mediated by nicotinamide adenine dinucleotide phosphate (NADPH) oxidase activation, which could be blocked by the pharmacological SGLT inhibitor phlorizin, but not by the glucose transporter type 1 or 4 (GLUT1/4) inhibitor phloretin (82). Indeed, knockdown of SGLT1 reduces myocardial nitro–oxidative stress and inflammation, and results in preservation of LV systolic and diastolic function (68, 73, 74). Furthermore, SGLT1 inhibition reduces Na+ overload in cardiomyocytes (67), which is a hallmark of failing cardiomyocytes.

Importantly, a growing body of evidence suggest that cardiac SGLT1 plays causal role in the development of HF. Cardiomyocyte–specific overexpression of SGLT1 for 10 weeks in non–diabetic mice is sufficient to induce HF, which could be reversed by SGLT1 knock down thereafter (79). Similarly, pathological overactivation of AMPK induces HF in an SGLT1–dependent manner (66, 79). Finally, mice with global SGLT1 knockout are protected from the development pathological LV hypertrophy in response

to chronic pressure overload induced by transverse aortic constriction (TAC) (71). While in small animal studies myocardial SGLT1 seems to contribute to the pathophysiology of HF, to date, there is limited evidence in humans with HF to reinforce this theory.

Apart from HF, a recent study showed that knock down of SGLT1 protected against acute myocardial ischemia–reperfusion injury in both *in vivo* and *ex vivo* settings, without affecting glucose uptake, resulting in reduced myocardial nitro–oxidative stress (68). While reducing infarct size is not equal to reducing the risk of myocardial infarction, it is notable that only the dual SGLT1/2 inhibitor sotagliflozin reduced the risk of myocardial infarction in patients with T2DM, but not selective SGLT2 inhibitors (83).

Taken together, increased expression of SGLT1 might contribute to the development and worsening of HF in small animals, albeit it is unclear whether this increase in expression is independent of the nature of the pathological stimuli that elicit HF. Furthermore, while on the population level reduced SGLT1 activity contributes to reduction in HF events, there is limited evidence in humans with HF to suggest a connection between the severity of HF and the level of myocardial SGLT1 expression. Even though SGLT2 inhibitors are now the cornerstone of HF drug therapy regardless of T2DM, the mechanism of action in incompletely understood. Given that these agents non–selectively block SGLT1 to different extent, it is clinically relevant to characterize myocardial SGLT1 expression in HF.

2. Objectives

We hypothesized that myocardial LV SGLT1 expression is significantly increased in HF and correlates with LV dilation and systolic dysfunction. We further hypothesized that such increase in LV SGLT1 expression can be comparably evoked in two pathologically distinct models of chronic hemodynamic overload–induced HF.

The objectives of the present studies were the following:

1) In patients with end–stage HF, we aimed to:
    a) characterize myocardial LV SGLT1 and SGLT2 expressions in conjunction with those of the other two major glucose transporters GLUT1 and GLUT4,
    b) assess possible regulators of myocardial SGLT1 expression, and
    c) establish the clinical relevance of the level of myocardial SGLT1 expression.
2) In two rat models of severe HF, we aimed to:
    a) characterize myocardial LV SGLT1 expression,
    b) assess possible regulators of myocardial SGLT1 expression, and
    c) establish the pathological relevance of the level of myocardial SGLT1 expression.

3. Methods

3.1. Study in patients with end–stage HF

3.1.1. Study population and sample procurement

Well–characterized, de–identified human myocardial tissue samples were obtained from the Transplantation Biobank of the Heart and Vascular Center, Semmelweis University, Budapest, Hungary (84, 85). The procedure of sample procurement was reviewed and approved by the institutional and national ethics committees (ETT TUKEB 7891/2012/EKU [119/PI/12.] and IV/10161-1/2020/EKU). Informed consent was obtained from patients in line with the Declaration of Helsinki prior to sample collection. In all cases, myocardial LV samples were surgically removed and immediately snap–frozen in liquid nitrogen under sterile conditions for molecular measurements, whereas LV samples for histological analyses were immediately conserved in 4% buffered paraformaldehyde. Control myocardial LV samples (n=9) were isolated from LV papillary muscles removed from patients undergoing mitral valve replacement (open procedure) due to mitral regurgitation. Myocardial LV samples from end–stage HF patients (n=71) were collected during orthotopic heart transplantation from the diseased hearts of the recipients immediately after explantation. Echocardiographic data registered prior to surgery were obtained from the database of our Transplantation Biobank, as were other baseline characteristics (age, sex, body mass index [BMI], medical and device therapies).

Out of LV samples from over 400 individual patients stored in the Transplantation Biobank, an overall of 80 LV samples (from separate patients) were included in the present study (based on the criteria below). End–stage HF patients were stratified into subgroups based on the etiology of HF, and whether cardiac resynchronization therapy (CRT) had been received up to the time of heart transplantation, as the latter has proven effect on signaling on the cardiomyocyte level (86). Importantly, patients on left ventricular assist device therapy (a type of mechanical circulatory support) were excluded from the present study.

Accordingly, the following groups were defined in our study who met the outlined criteria:

1. non–failing controls (n=9): preserved LV systolic function
2. end–stage HF patients not receiving CRT (n=44):
    a. hypertrophic cardiomyopathy (HCM, n=7): severe LV hypertrophy; absence of relevant comorbidities (hypertension, T2DM); no relevant coronary atherosclerosis
    b. dilated cardiomyopathy (DCM, n=12): severe LV dilation not explained by valvular disease; no history of myocarditis; no relevant comorbidities (hypertension, T2DM); no relevant coronary atherosclerosis
    c. ischemic heart disease (IHD, n=14): severe diffuse coronary atherosclerosis at multiple sites, with or without prior revascularization therapy; no T2DM as comorbidity
    d. ischemic heart disease and T2DM (IHD–T2DM, n=11): severe diffuse coronary atherosclerosis at multiple sites, with or without prior revascularization therapy; T2DM as comorbidity
3. end–stage HF patients receiving CRT (n=27):
    a. DCM with CRT (CRT:DCM, n=9): severe LV dilation not explained by valvular disease; no history of myocarditis; no relevant comorbidities (hypertension, T2DM); no relevant coronary atherosclerosis
    b. IHD with CRT (CRT:IHD, n=9): severe diffuse coronary atherosclerosis at multiple sites, with or without prior revascularization therapy; no T2DM as comorbidity
    c. IHD and T2DM, with CRT (CRT:IHD–T2DM, n=9): severe diffuse coronary atherosclerosis at multiple sites, with or without prior revascularization therapy; T2DM as comorbidity

Prior to cardiac surgery, echocardiographic measurements were performed on various echocardiographic platforms. Left ventricular end–diastolic diameter (LVEDD, mm) was quantified as a marker of LV dilation, a hallmark of LV adverse remodeling. This parameter was measured in M-mode or directly in 2D in the parasternal long axis view.

Left ventricular systolic function was determined by LV EF (%) using Teicholz or Simpson methods.

3.2. Study in rats with severe HF

3.2.1. Experimental animals

A total of 48 male Wistar rats (purchased from Toxi–Coop; Budapest, Hungary) were kept under standard conditions (22 ± 2 °C with 12 h light/dark cycles) and were allowed access to laboratory rat chow and water ad libitum during the experimental period. Prior to experimentations, rats were allowed to acclimatize for one week. The present investigation conformed to the EU Directive 2010/63/EU and to the Guide for the Care and Use of Laboratory Animals published by the US National Institutes of Health (NIH Publication No. 85–23, revised 1996). The study was approved by the Scientific Ethical Committee on Animal Experimentation (Hungary) and by the Institutional Ethics Committee of Semmelweis University (Reference No. PEI/001/2374–4/2015).

3.2.2. Rat models of severe HF

Model of pressure–overload induced HF: Three–week–old (bodyweight: 50–100g) male Wistar rats underwent transverse aortic constriction (TAC) to induce chronic progressive pressure overload for ~14 weeks resulting in HF. Anesthesia was induced by placing the animals in a chamber filled with 5% isoflurane. Then, animals were intubated, and anesthesia was maintained with a small animal respirator using 2% isoflurane (mixed in pure oxygen). Core temperature (37 ± 0.5°C) was kept constant by placing the rats in a supine position on a controlled heating pad. Left anterolateral thoracotomy was performed in the second intercostal space; next, the aortic arch was isolated and constricted to match the size of the external diameter of a 21–gauge needle between the innominate artery and the left common carotid artery. Finally, the thorax was closed and the skin layers were sutured. The wound was carefully disinfected, tramadol (10 mg/kg) and physiological saline were subcutaneously injected shortly after weaning the animals off the respirator. Age and sex–matched control animals (Sham–T) underwent the same procedure as above, except the aortic arch was not constricted (i.e., no pressure overload).

Model of volume–overload induced HF: Six–week–old (bodyweight: 150–200g) male Wistar rats underwent shunting of the abdominal aorta and the inferior vena cava (creating an aortocaval fistula, ACF) to induce chronic progressive volume overload for ~24 weeks resulting in HFAs described above, anesthesia was induced and maintained, whereas core temperature was kept constant. A midline laparotomy was performed and after exposing the abdominal aorta and the inferior vena cava, both vessels were clipped transiently distal to the origin of the left renal artery and proximal to the aortic bifurcation. Then, in this isolated section, the anterior aortic wall was punctured using a 18–gauge needle, which was then advanced through the adjacent venous wall, creating an ACF. Following the establishment of the shunt, the needle was withdrawn and the puncture on the surface of the aorta was sealed using a drop of cyanoacrylate glue. When the ACF was secured, the intestines were replaced, the abdominal muscle layers were sutured, followed by closure of the skin incision. The above disinfection and analgesic measures were applied. Age and sex–matched control animals (Sham–A) underwent the same procedure as above, except ACF was not created (i.e., no volume overload).

3.2.3. Experimental groups

Based on the above, our rat study comprised four experimental groups:

1. Sham–T (n=12): rats undergoing sham operation as controls of TAC and followed for 14 weeks
2. TAC (n=12): rats undergoing TAC and followed for 14 weeks
3. Sham–A (n=12): rats undergoing sham operation as controls of ACF and followed for 24 weeks
4. ACF (n=12): rats undergoing ACF operation and followed for 24 weeks

3.2.4. Echocardiographic measurements in rats

The Vivid I (GE Healthcare, Waukesha, WI, USA) echocardiographic imaging system equipped with the GE 12L–RS linear transducer (13 MHz) was used to non–invasively assess the temporal alterations in LV structure and function. Prior to measurements, rats were anesthetized in a chamber with 5% isoflurane, then anesthesia was maintained by inhalation of 2% isoflurane (mixed in pure oxygen) from an insulated facemask, while

placing the rats in a supine position on a controlled heating pad (maintaining core temperature at 37 ± 0.5°C throughout the measurements). In order to optimize the acoustic window, the thorax was thoroughly shaved. Images were captured in two–dimensional parasternal long–axis and short–axis views at the mid–papillary level. The digital images were analyzed offline using EchoPac (GE Healthcare). The following parameters were obtained from the average of three consecutive cardiac cycles (devoid of breathing movements): LVEDD, LV end–systolic diameter (LVESD), anterior wall thicknesses (AWT) and posterior wall thicknesses (PWT) in diastole (d) and systole (s). Then, LV mass was quantified using the Devereux formula: $0.8\times(1.04\times((LVEDD+AWT+PWT)^3-LVEDD^3))+0.6$.

3.2.5. Left ventricular pressure–volume analysis in rats and sample procurement

Left ventricular pressure–volume (PV) analysis was performed. In brief, rats were anesthetized in a chamber filled with 5% isoflurane, then following tracheotomy and intubation, anesthesia was maintained by artificial ventilation of 1.5% isoflurane (mixed in pure oxygen). For fluid administration, the left external jugular vein was cannulated. Thereafter, rocuronium bromide (2 mg/kg bodyweight) was administered intraperitoneally to achieve generalized muscle relaxation. A 2F microtip pressure–conductance catheter (SPR–838; Millar Instruments, Houston, TX, USA) was advanced into the ascending aorta through the right common carotid artery. Following stabilization, the catheter was guided into the LV under pressure control. The following parameters were obtained using a PV analysis software (PVAN; Millar Instruments): heart rate, LV end–systolic pressure (LVESP), and time constant of LV pressure decay (Tau). Then, the slope of the end–systolic PV relationship (ESPVR) – a relatively load independent contractility index – was calculated from PV loops registered while transiently reducing preload (achieved by transient occlusion of the inferior vena cava). For analysis, all PV loops were acquired with the ventilator turned off for 5s and the animal apneic (due to generalized muscle relaxation). Then, volume calibration was performed by calculating parallel conductance.

Animals were euthanized at the end of the PV protocol, followed by cannulation of the abdominal aorta. After collection of arterial blood, cold (4°C) 50 mL Ringer solution was infused retrogradely. After the washout, hearts were excised and weighed, midpapillary cross–sections were obtained and stored in 4% buffered paraformaldehyde

(for immunohistochemical analyses). Other parts of the LV were instantly snap–frozen in liquid nitrogen and stored at –80°C (for molecular measurements). Tibial length and lung weights were measured post–mortem.

3.3. Molecular measurements on human and rat heart samples

3.3.1. Myocardial LV RNA isolation and quality control

Myocardial RNA isolation was performed identically in human and rat heart samples.

Myocardial LV tissue samples (~25 mg) were homogenized in Buffer RLT (Qiagen, Netherlands) using Bertin Precellys 24 Tissue Homogenizer with Bertin Cryolys cooling system (Bertin Technologies, France) to ensure adequate and constant cooling (~0°C) of samples throughout the procedure. Then, total RNA was isolated using RNeasy Fibrous Tissue Kit (Qiagen) as per the manufacturer's protocol. RNA concentration was measured photometrically at 260 nm, while RNA purity was ensured by obtaining 260/280 nm and 260/230 nm optical density ratio of ~ 2.0, respectively.

In myocardial samples of human hearts, we additionally analyzed the quality of the isolated RNA. This is because the procedure of sample procurement is more heterogenous in case of human hearts due to variable intraoperative conditions (e.g. disparities in duration of time without proper cooling of the samples). This could produce erroneous differences in expression of certain targets. Therefore, to rule out that differences in expression of targets is caused by differences in the quality of samples, we loaded each individual human LV RNA sample onto Agilent 6000 Pico LabChips (Agilent Technologies, Santa Clara, CA, USA) and performed analyses using Agilent 2100 Bioanalyzer. Based on the ratio of 18S/28S rRNA in the electrophoretogram of each sample, an RNA Integrity Number (RIN) was assigned (ranging from RIN 0–10, higher RIN values indicate excellent RNA quality) to each sample. The RIN of samples homogenized from intraoperatively obtained human tissues typically range from ~6.0–8.0 when efforts are made to prevent degradation (87).

3.3.2. RNA reverse transcription and quantitative real–time polymerase chain reaction

Reverse transcription of RNA to cDNA was conducted with QuantiTect Reverse Transcription Kit (Qiagen) by using 1µg RNA of each sample and random primers, as per protocol. Then, quantitative real–time polymerase chain reaction (qRT–PCR) was performed on StepOnePlus RT PCR System (Thermo Fisher Scientific, Waltham, MA, USA) using TaqMan Universal PCR MasterMix and TaqMan Gene Expression Assays (Thermo Fisher Scientific) for specific targets.

1. In LV heart samples obtained from human subjects, relative mRNA expressions of the following targets were quantified: Solute Carrier Family 5 Member 1 (SLC5A1 encoding SGLT1; ID: Hs01573793_m1); SLC5A2 (encoding SGLT2; assay ID: Hs00894642_m1); SLC2A1 (encoding GLUT1; assay ID: Hs00892681_m1); SLC2A4 (encoding GLUT4; assay ID: Hs00168966_m1); and the housekeeping glyceraldehyde–3–phosphate dehydrogenase (GAPDH; assay ID: Hs99999905_m1).
2. In LV heart samples obtained from rats, relative mRNA expressions of the following targets were quantified: pathological hypertrophy markers β and α–myosin heavy chain (β/α–MHC; β–MHC assay ID: Rn00568328_m1; α–MHC assay ID: Rn00568304_m1), and pro–fibrotic markers, including transforming growth factor–β (TGF–β; assay ID: Rn00572010_m1), connective tissue growth factor (CTGF; assay ID: Rn01537279_g1), and collagen type I alpha 1 (Col1a1; assay ID: Rn01463848_m1), and the housekeeping GAPDH (assay ID: Rn01775763_g1).

Every sample was quantified in duplicates or triplicates in a volume of 10µl in each well containing 1µl cDNA. Data were normalized to the housekeeping GAPDH, then to a positive calibrator (pool of cDNA from all samples of the DCM group in case of human samples, and of the Sham groups in case of rat samples) in each case. Accordingly, gene expression levels were calculated using the comparative method ($2^{-\Delta\Delta CT}$).

3.3.3. Protein isolation and western blotting

Myocardial LV tissue samples (~25 mg) were homogenized in RIPA buffer (Bio–Rad Laboratories, Hercules, CA, USA) containing protease and phosphatase inhibitor cocktail (Roche, Basel, Switzerland), using Bertin Precellys 24 Tissue Homogenizer with Bertin Cryolys cooling system (Bertin Technologies). The concentrations of the extracted proteins were measured by BCA assay (Thermo Fisher Scientific). Then, protein homogenates were suspended in sample buffer and heated at 70–100°C for 5–10 min. A total of 40μg protein for each sample was loaded onto 6–12% acrylamide gels and separated with sodium dodecyl sulphate polyacrylamide gel electrophoresis system (Bio–Rad Laboratories). Gels were transferred to polyvinylidene difluoride membranes under dry conditions. Membranes were then washed and blocked for 1 hour in 5 % bovine serum albumin in Tris–buffered saline Tween 20 (TBST) at room temperature. Next, membranes were incubated overnight at 4°C with the primary antibodies (diluted in 2.5% bovine serum albumin in TBST) against specific targets (purchased from Cell Signaling Technology, Danvers, MA, USA, or Abcam, Cambridge, UK).

1. In LV heart samples obtained from human subjects, relative protein expressions of the following targets were quantified: SGLT1 (1:1000; ID: #5042); phosphorylated adenosine–monophosphate–activated protein kinase α catalytic subunit (P–AMPKα, Thr172) (1:1000; ID: #2535); total–AMPKα (1:1000; ID: #2532); phosphorylated extracellular signal–regulated protein kinase 1/2 (P–ERK1/2, Thr202/Tyr204) (1:1000; ID: #9101); total–ERK1/2 (1:1000; ID: #9102) and the housekeeping GAPDH (1:5000; ID: #5174).
2. In LV heart samples obtained from rats, relative protein expressions of the following targets were quantified: SGLT1 (ID: #5042); NADPH oxidase 4 (Nox4; ID: ab133303); P–AMPKα (Thr172; ID: #2535); total–AMPKα (ID: #2532); P–ERK1/2 (Thr202/Tyr204; ID: #9101); total–ERK1/2 (ID: #9102); and anti–phosphorylated acetyl coenzyme–A carboxylase (P–ACC, Ser79; ID: #3661).

The blots were washed and incubated with horseradish peroxidase–conjugated secondary antibody (1:5000, 2.5% bovine serum albumin in TBST) for 1 hour at room temperature. The immunoreactive protein bands were developed using Super Signal

West Pico Plus (Thermo Fisher Scientific) chemiluminescent substrate. The intensity of the immunoblot bands was analyzed with Bio–Rad Image Lab Software 6.0 (Bio–Rad Laboratories). Within each sample, the intensity of the bands of the primary targets was normalized to that of the housekeeping GAPDH on the same blot.

3.3.4. Histology and immunohistochemistry

All samples were fixed in 4% buffered paraformaldehyde for ~24h, and then were embedded in paraffin, and 5–7 μm thick sections were cut.

In case of human heart samples, after deparaffination and antigen retrieval, sections were incubated with anti–SGLT1 antibody (1:100; overnight, 4°C; ab14686). HRP–conjugated secondary antibody (30 min, room temperature) and black colored nickel–cobalt enhanced diaminobenzidine (6 min, room temperature) were used to visualize the labeling. Light microscopic examination was performed using Nikon Eclipse Ni Microscope (Nikon Instruments, Amstelveen, Netherlands) and a digital image was captured in each section (from each patient) using Nikon DS–RI2 camera (Nikon Instruments) with 40x dry objective. Immunofluorescent staining was performed after deparaffination and antigen retrieval using anti–SGLT1 antibody (1:100; overnight at 4 °C; ab14686). Alexa–Fluor 488 conjugated goat anti–rabbit IgG (1:500; 30 min, room temperature; ab150077) served as secondary antibody. Sodium–potassium ATPase (Na–K–ATPase) was labeled by anti–alpha 1 Na–K–ATPase antibody (1:200, 2 hours, room temperature; ab7671), where Alexa–Fluor 568 goat anti–mouse IgG (1:500; 30 min, room temperature; ab175473) was used for visualization. Then, slides were covered by 4’,6–diamidino–2–phenylindole (DAPI)–containing mounting medium (Vectashield; Vector Laboratories, Burlingame, CA, USA). Representative images were acquired by Nikon Eclipse A1 Confocal Laser Microscope (Nikon Instruments) using a 40x dry objective. All antibodies used for immunohistochemical measurements in human heart samples were purchased from Abcam, Cambridge, UK.

In case of rat heart samples, following deparaffinization, endogenous peroxidase activity was blocked by 3% H_2O_2, and 2.5% normal horse serum (Vector Laboratories, Burlingame, CA, USA) was used to prevent non–specific labeling. After overnight incubation with the rabbit polyclonal anti–3–nitrotyrosin (3–NT, nitrosative stress marker) antibody (1:500, Merck Millipore, Burlington, MA, USA) or the rabbit

polyclonal anti–4–hydroxy–2–nonenal (4–HNE, oxidative stress marker) (1:100, Abcam, Cambridge, UK) antibody at 4 °C, secondary labeling was achieved by HRP–linked anti–rabbit polyclonal horse antibodies (Vector Laboratories), which was visualized by brown–colored diamino–benzidine (Vector Laboratories). Images of the immunolabeled LV tissue sections were captured by Nikon Eclipse Ni Microscope (Nikon Instruments, Amstelveen, Netherlands) with 20x objective lens, using a Nikon DS–RI2 camera (Nikon Instruments) and NIS–Elements BR imaging software (Nikon Instruments). The percentage of positively stained tissue area compared to the total tissue area was measured with ImageJ Software (National Institutes of Health, Bethesda, MA, USA). Following image analysis, blue–colored hematoxylin (Vector Laboratories) was utilized as counterstaining, after which representative images were captured. Additionally, in separate staining procedures, hematoxylin–eosin staining was performed to visualize cellular structure in rat heart samples.

3.4. Statistical analysis

Values are expressed as mean ± standard error of the mean (SEM) for continuous variables, whereas categorical variables are expressed as frequencies and percentages. The assumption of normal distribution of the data was analyzed using the Shapiro–Wilk test and the predicted probability plots. In case of the study in humans, when the assumption of normal distribution was violated, log2–transformed data were used. The assumptions of normal distribution and homoscedasticity of the residuals were analyzed by plotting the predicted values and residuals on scatter plots. Significance of difference between two groups was assessed using unpaired Student *t*–test with Welch's correction (in both human and rat studies) or using the non–parametric Mann–Whitney *U* test (only in case of the study in rats).

In the human study, one–way analysis of variance (ANOVA) was performed with Welch's correction followed by Dunnett T3 post hoc test to compute intergroup differences relative to the Control group when more than two groups were analyzed. Analysis of covariance (ANCOVA) was performed to quantify the observed differences after adjusting for age, sex, and BMI. The assumption of homogeneity of regression slopes was not violated in any case as indicated by non–significant interaction between the covariates and the fixed factor. Also, substantial collinearity among the predictor

variables was not an issue as variance inflation factors (VIF) were <5.00 in all cases. Reported P values associated with bias–corrected and accelerated (BCa) 95% confidence intervals (CI) based on n=1000 bootstrap samples were adjusted for multiple comparisons using Bonferroni correction.

To analyze the temporal development of LV hypertrophy (LV mass) in the rat models of HF, mixed–effects ANOVA was conducted without assuming sphericity, including hypothesis testing for the following factors: type of surgery (P_{TAC} or P_{ACF} versus respective Sham); time (P_{time}); and their interaction (P_{int}). Post hoc analyses at different time–points between the operated and respective sham groups were conducted using Bonferroni correction.

In all cases, Spearman's *rho* (r_s) was computed for zero–order correlation analysis. In case of the human study, we estimated that at two–tailed α=0.05 and power (β) of 80%, in order to detect a medium effect size with partial correlation analysis based on 4 predictors, a sample size of n=55 is required. Accordingly, partial correlation analysis was performed on ranked scores to compute correlation coefficients adjusted for age, sex, and BMI. For all correlation coefficients in the human study, BCa 95% CI are reported based on n=1000 bootstrap samples. Point–biserial correlation analysis on ranked scores was performed to compute the overall effect of CRT on LV mRNA expression of target genes.

Statistical analyses were carried out using IBM SPSS Statistics 25 (IBM, Armonk, NY, USA) and GraphPad Prism 8 (GraphPad Software, San Diego, CA, USA), the latter was also used to graph data. In all cases, the untransformed, original datapoints are graphed. For hypothesis testing, a two–tailed P<0.050 value was defined as the threshold for statistical significance. In the figures, the levels of significance are depicted using asterisks (*=P<0.050, **=P<0.010, ***=P<0.001).

4. Results

4.1. Study in patients with end–stage HF

4.1.1. Study populations

Patient and clinical characteristics in each group are provided in Table 2. Overall, 8 groups of patients were included in the study, one group served as non–failing control and 7 groups had severe HF. As seen in Table 2, controls had preserved LV systolic function (EF=61.2±3.4%), while patients with HF, including those with HCM, presented with substantially reduced EFs. All study groups had a mean RIN >7.9, indicating excellent RNA quality of samples (Table 2).

4.1.2. Left ventricular mRNA expression profiles of SGLT1, SGLT2, GLUT1 and GLUT4

Myocardial LV mRNA expression of SGLT1 significantly differed among different types of HF (ANOVA P=0.004) (Figure 2A). Pairwise comparisons between the control group and the HF groups revealed that SGLT1 was significantly upregulated in patients with DCM (P=0.007), but not with HCM (P=0.831) (Figure 2A). Those with IHD also had a significantly increased SGLT1 expression irrespective of T2DM (P<0.05, respectively) (Figure 2A). According to ANCOVA, differences in LV SGLT1 expression persisted even after adjusting for age, sex, and BMI (P=0.024). Patients with DCM (P=0.020) or IHD (P=0.040) had significantly increased SGLT1 expression compared to controls, while there was a strong tendency in case of the IHD–T2DM group (P=0.056).

No detectable LV SGLT2 mRNA expression was found in any of the studied groups.

LV mRNA expression of GLUT1 also differed significantly among the studied groups (ANOVA P=0.011) (Figure 2B). Patients with DCM, IHD and IHD–T2DM had a significantly increased GLUT1 expression as compared with controls (P<0.05, respectively), but not those with HCM (P=1.000) (Figure 2B). ANCOVA revealed that GLUT1 was still significantly different among the groups after adjusting for age, sex, and BMI (P=0.035). However, intergroup differences were not statistically significant. Finally, GLUT4 expression was comparable among the groups (ANOVA P=0.131) (Figure 2C), even after adjusting for age, sex, and BMI (ANCOVA P=0.544).

Table 2. Patient baseline characteristics and RNA integrity numbers of myocardial left ventricular RNA samples according to subgroups

BMI: body mass index; CRT: cardiac resynchronization therapy; DCM: dilated cardiomyopathy; EF: left ventricular ejection fraction; F: female; HCM: hypertrophic cardiomyopathy; IHD: ischemic heart disease; LVEDD: left ventricular end–diastolic diameter; RIN: RNA integrity number; T2DM: type 2 diabetes mellitus

	Control (n=9)	**HCM (n=7)**	**DCM (n=12)**	**IHD (n=14)**	**IHD–T2DM (n=11)**	**CRT: DCM (n=9)**	**CRT: IHD (n=9)**	**CRT: IHD–T2DM (n=9)**
Age (years)	68.6 ± 1.9	36.6 ± 4.4	46.8 ± 3.4	58.7 ± 1.4	57.0 ± 1.4	47.7 ± 4.1	59.0 ± 1.6	60.1 ± 1.6
Sex (F, %)	8/9 (89%)	4/7 (57%)	2/12 (17%)	5/12 (36%)	3/11 (27%)	3/9 (33%)	0/9 (0%)	2/9 (22%)
BMI (kg/m^2)	26.1 ± 1.6	25.5 ± 1.9	25.7 ± 1.6	26.5 ± 0.8	27.9 ± 0.9	23.5 ± 1.0	27.7 ± 1.6	30.0 ± 1.1
LVEDD (mm)	53.2 ± 4.0	50.7 ± 4.6	73.4 ± 2.6	69.9 ± 2.7	63.9 ± 2.7	76.2 ± 3.8	70.6 ± 6.2	70.0 ± 3.6
EF (%)	61.2 ± 3.4	36.9 ± 4.6	21.9 ± 1.1	27.3 ± 1.4	22.9 ± 1.9	19.3 ± 2.7	19.7 ± 2.4	23.3 ± 2.4
Years with CRT	–	–	–	–	–	2.9 ± 0.6	3.2 ± 1.8	3.4 ± 0.8
Beta blocker	8/9 (89%)	5/7 (71%)	9/12 (75%)	11/14 (79%)	4/11 (36%)	2/9 (22%)	8/9 (89%)	8/9 (89%)
Renin–angiotensin system inhibitor	1/9 (11%)	0/7 (0%)	7/12 (58%)	11/14 (79%)	9/11 (82%)	3/9 (33%)	7/9 (78%)	8/9 (89%)
Mineralo–corticoid receptor antagonist	2/9 (22%)	4/7 (57%)	9/12 (75%)	13/14 (89%)	8/11 (73%)	6/9 (67%)	8/9 (89%)	6/9 (67%)
Diuretic	4/9 (44%)	4/7 (57%)	10/12 (83%)	11/14 (79%)	7/11 (64%)	7/9 (78%)	7/9 (78%)	6/9 (67%)
Statin	3/9 (33%)	0/7 (0%)	2/12 (17%)	7/14 (50%)	6/11 (55%)	0/9 (0%)	4/9 (44%)	8/9 (89%)
Metformin	–	–	–	–	6/11 (55%)	–	–	5/9 (55%)
Insulin	–	–	–	–	3/11 (27%)	–	–	1/9 (11%)
RIN	9.3 ± 0.1	8.3 ± 0.4	8.4 ± 0.3	8.1 ± 0.4	8.2 ± 0.3	7.9 ± 0.3	8.0 ± 0.3	7.9 ± 0.3

continuous variables: mean ± SEM; categorical variables: counts and percentages

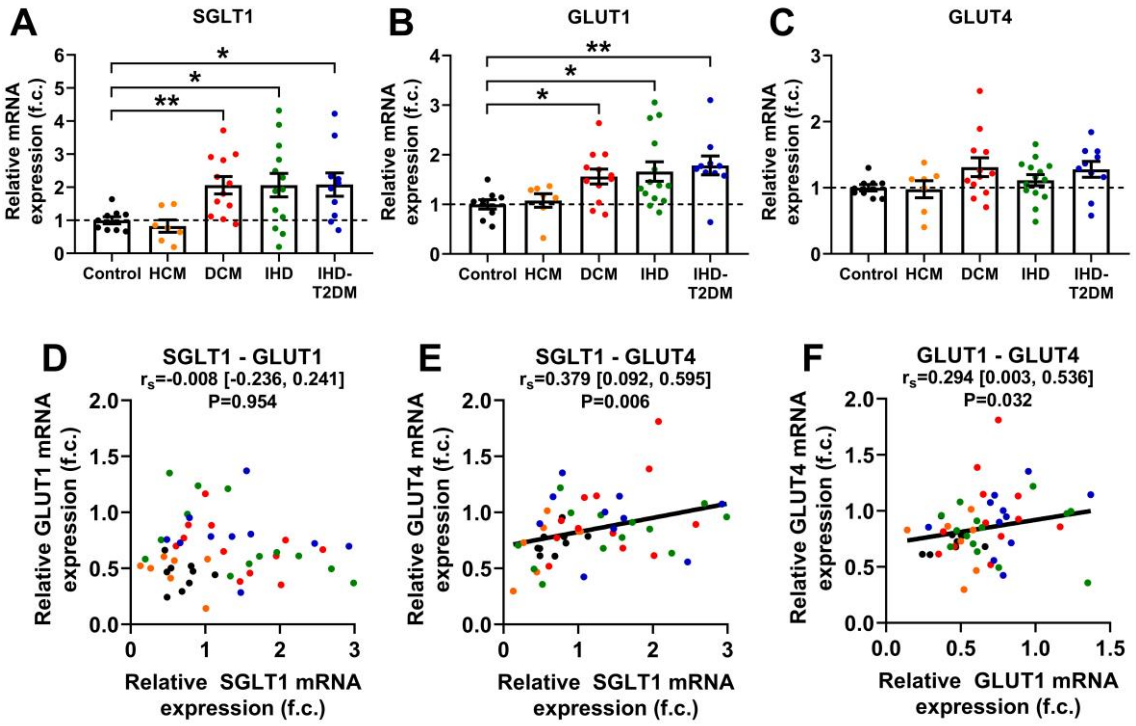

Figure 2. Myocardial left ventricular mRNA expressions of SGLT1, GLUT1, and GLUT4, and their correlations in human heart samples

A–C: *Quantification of left ventricular relative mRNA expressions of SGLT1, GLUT1, and GLUT4 in controls and in patients with end–stage heart failure.*
D–F: *Correlation between left ventricular relative mRNA expressions of SGLT1, GLUT1, and GLUT4, respectively. Color codes represent HF subtypes seen in Figure 2A–C.*

DCM: dilated cardiomyopathy; f. c. fold change; GLUT1/4: glucose transporter type 1/4; HCM: hypertrophic cardiomyopathy; IHD: ischemic heart disease; IHD–T2DM: IHD and type 2 diabetes mellitus; SGLT1: sodium–glucose cotransporter 1

4.1.3. Correlation of LV mRNA expressions of SGLT1, GLUT1, and GLUT4

Despite being similarly upregulated, LV mRNA expression of SGLT1 did not significantly correlate with that of GLUT1 (r_s=–0.008, P=0.954) (Figure 2D), even after adjusting for age, sex, and BMI (r=–0.060, P=0.693). However, GLUT4 mRNA expression correlated positively with SGLT1 (r_s=0.379, P=0.006) (Figure 2E) and GLUT1 (r_s=0.294, P=0.032) expressions (Figure 2F), respectively. These remained comparable in adjusted models (GLUT4–SGLT1: r=0.324, P=0.030; GLUT4–GLUT1: r=0.254, P=0.085).

4.1.4. Correlation of LV mRNA expressions of SGLT1, GLUT1, and GLUT4 with LV dilation and systolic function

LV SGLT1 mRNA expression showed a significant positive correlation with LVEDD (r_s=0.493, P<0.001), a marker of LV dilation (Figure 3A). Furthermore, SGLT1 expression correlated negatively with LV EF (r_s=–0.477, P<0.001) (Figure 3B), a marker of LV systolic function. Partial correlation analysis on ranked scores revealed that after adjusting for age, sex, and BMI, SGLT1 mRNA expression remained significantly correlated with LVEDD (r=0.476, P=0.002) and LV EF (r=–0.542, P<0.001), respectively.

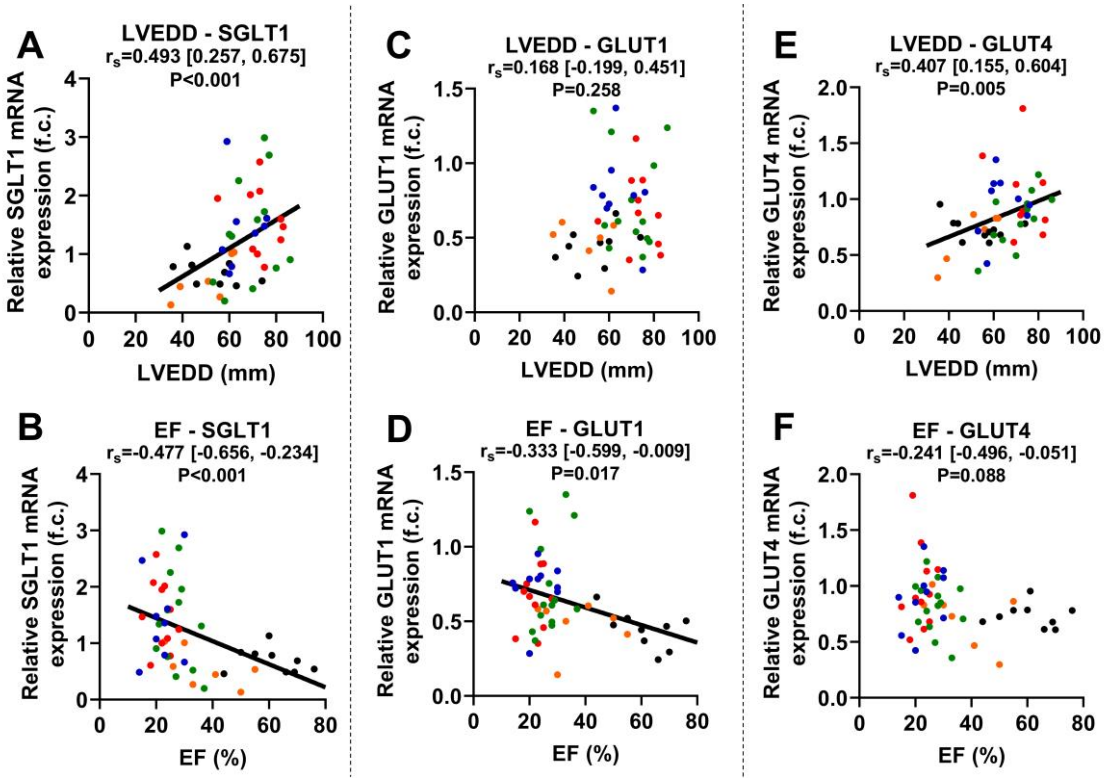

Figure 3. Correlation between left ventricular glucose transporter mRNA expressions and echocardiographic parameters in human hearts

A–B: *Correlation between LVEDD and LV EF with LV mRNA expression of SGLT1.*
C–D: *Correlation between LVEDD and LV EF with LV mRNA expression of GLUT1.*
E–F: *Correlation between LVEDD and LV EF with LV mRNA expression of GLUT4.*
Color codes represent HF subtypes seen in Figure 2A–C.

EF: ejection fraction; f. c.: fold change; GLUT1/4: glucose transporter type 1/4; HF: heart failure; LV: left ventricular; LV: left ventricular; LVEDD: left ventricular end–diastolic diameter; SGLT1: sodium–glucose cotransporter 1

LV GLUT1 mRNA expression showed significant inverse correlation with EF (r_s=–0.333, P=0.017) (Figure 3D) but did not correlate with LVEDD (Figure 3C). On the contrary, GLUT4 expression correlated significantly with LVEDD (r_s=0.407, P=0.005) (Figure 3E), but only tendentially with EF (r_s=–0.241, P=0.088) (Figure 3F). However, after adjusting for age, sex, and BMI, neither GLUT1 nor GLUT4 mRNA expression correlated significantly with LVEDD (GLUT1: r=–0.036, P=0.819; GLUT4: r=0.204, P=0.195) or EF (GLUT1: r=–0.147, P=0.331; GLUT4: r=–0.141, P=0.350).

3.1.5. Protein expression of SGLT1 and phosphorylation of ERK1/2 and AMPKα in human heart samples

Western blot analysis revealed that SGLT1 protein expression was significantly upregulated in patients with DCM, IHD, and IHD–T2DM (all P<0.05) compared to controls, but not in those with HCM (Figure 4A). LV SGLT1 protein expression showed a significant positive correlation with LVEDD (r_s=0.411, P=0.008) and a negative one with EF (r_s=–0.583, P<0.001) (Figure 4D), similarly to mRNA expression.

The phosphorylation of ERK1/2 on its activation sites (Thr202/Tyr204) was significantly downregulated in patients with DCM, IHD and IHD–T2DM (all P<0.05) compared to controls, showing a reciprocal change in contrast to SGLT1 protein expression (Figure 4B).

Compared to controls, the activating phosphorylation of AMPKα on Thr172 was numerically upregulated in patients with DCM and IHD, without reaching statistical significance (Figure 4C). However, AMPKα phosphorylation was significantly increased in patients with IHD–T2DM (P=0.036) (Figure 4C).

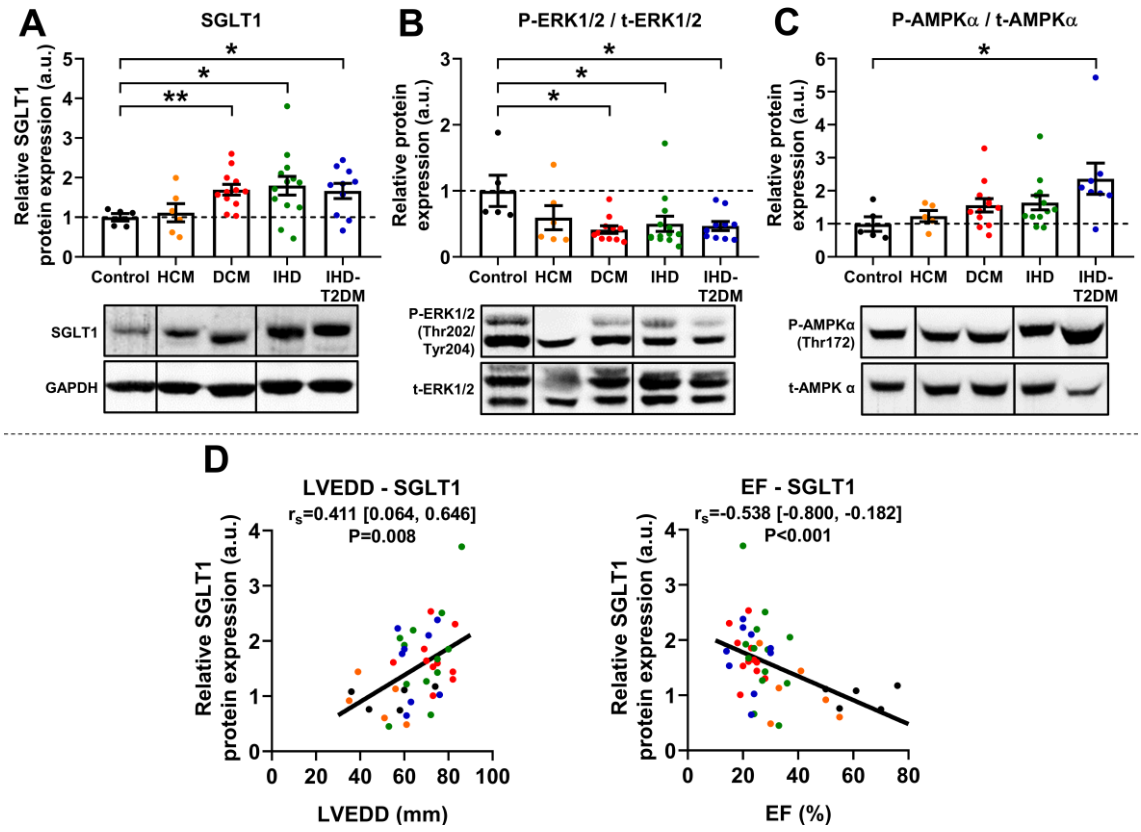

Figure 4. Left ventricular protein expressions of SGLT1, ERK1/2, and AMPKα in human heart samples

A–C: *Relative protein expressions of left ventricular SGLT1, phosphorylated ERK 1/2 (P–ERK1/2) versus total ERK1/2 (t–ERK1/2), and phosphorylated AMPKα (P–AMPKα) versus total AMPKα (t–AMPKα) in controls and in patients with HF, respectively.*
D: *Correlations between relative SGLT1 protein expression and LVEDD, and EF, respectively. Color codes represent HF subtypes seen in Figure 4A–C.*

AMPKα: adenosine–monophosphate–activated protein kinase α catalytic subunit; a.u.: arbitrary units; DCM: dilated cardiomyopathy; EF: ejection fraction; ERK1/2: extracellular signal–regulated kinase 1/2; HCM: hypertrophic cardiomyopathy; LVEDD: left ventricular end–diastolic diameter; IHD: ischemic heart disease; IHD–T2DM: IHD and type 2 diabetes mellitus; SGLT1: sodium–glucose cotransporter 1

4.1.6. Histological assessment of myocardial SGLT1 in human samples

A representative LV epicardial histological section from a patient with DCM stained against SGLT1 is shown in Figure 5A. The brownish staining of SGLT1 was predominantly confined to cardiomyocytes and an epicardial vessel, whereas the staining of fibrotic and adipose tissues was negligible. A similar pattern was seen in sections from patients in each study group (Figure 5B). Immunofluorescent staining of SGLT1 showed that its localization corresponded to that of Na–K–ATPase (Figure 5C).

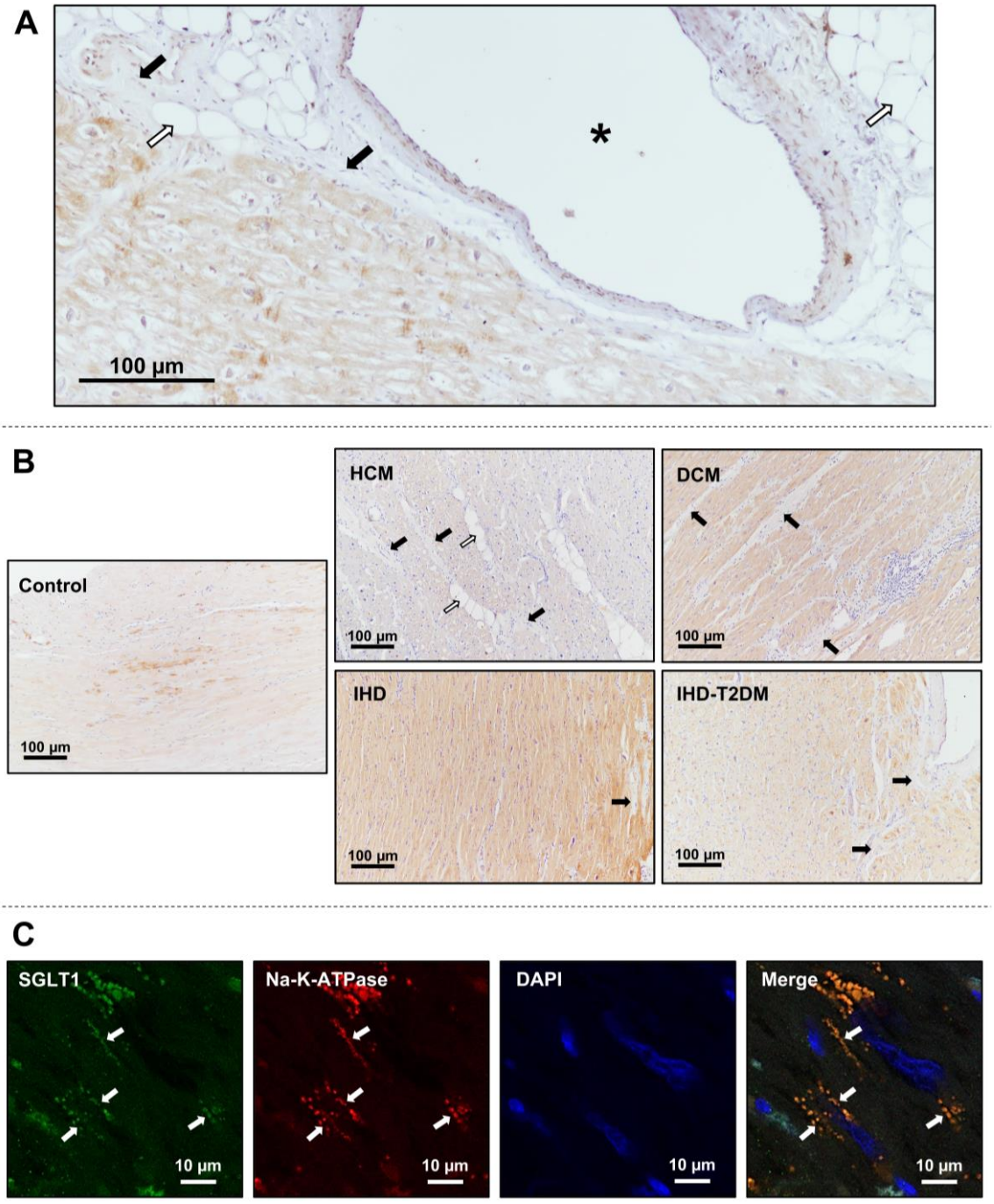

Figure 5. Immunohistochemical analysis of SGLT1 protein in the human heart

A: *Representative LV epicardial section from a patient with DCM.*
B: *Representative LV sections from patients within each study group.*
C: *Representative LV immunofluorescent sections from a patient with DCM.*

DAPI: 4',6–diamidino–2–phenylindol; DCM: dilated cardiomyopathy; HCM: hypertrophic cardiomyopathy; IHD: ischemic heart disease; IHD–T2DM: IHD and type 2 diabetes mellitus; LV: left ventricular; Na–K–ATPase: sodium–potassium ATPase; SGLT1 sodium–glucose cotransporter 1

4.1.7. Effect of CRT on the expression of SGLT1, GLUT1 and GLUT4

We investigated the effect of CRT on mRNA expression of SGLT1, GLUT1 and GLUT4 in LV samples from patients with DCM, IHD and IHD–T2DM. Overall, CRT was associated with significantly reduced LV SGLT1 expression (P=0.045) (Figure 6A). When comparing HF patients within the same etiological subgroup, we found that CRT was associated with significantly decreased SGLT1 mRNA expression in DCM patients compared to those not receiving CRT (P=0.026) (Figure 6A). According to ANCOVA, this difference remained significant even after adjusting for age, sex, and BMI (P=0.048). SGLT1 mRNA expression was comparable among IHD patients with and without CRT, irrespective of T2DM (Figure 6A), even after adjusting for age, sex, and BMI (IHD vs. CRT:IHD: P=0.642; IHD–T2DM vs. CRT:IHD–T2DM: P=0.576).

In line with mRNA expression, LV SGLT1 protein expression was significantly reduced in CRT:DCM patients, as compared with DCM patients not on CRT (P=0.029) (Figure 6D). The reciprocal upregulation of ERK1/2 phosphorylation was present in these patients (P=0.045) (Figure 6E), as well.

CRT was not associated with significant differences in GLUT1 mRNA expression among DCM, IHD and IHD–T2DM patients (Figure 6B). Similarly, GLUT4 expression was not significantly affected by CRT in any of the above groups (Figure 6C). These remained true even after adjusting for age, sex, and BMI.

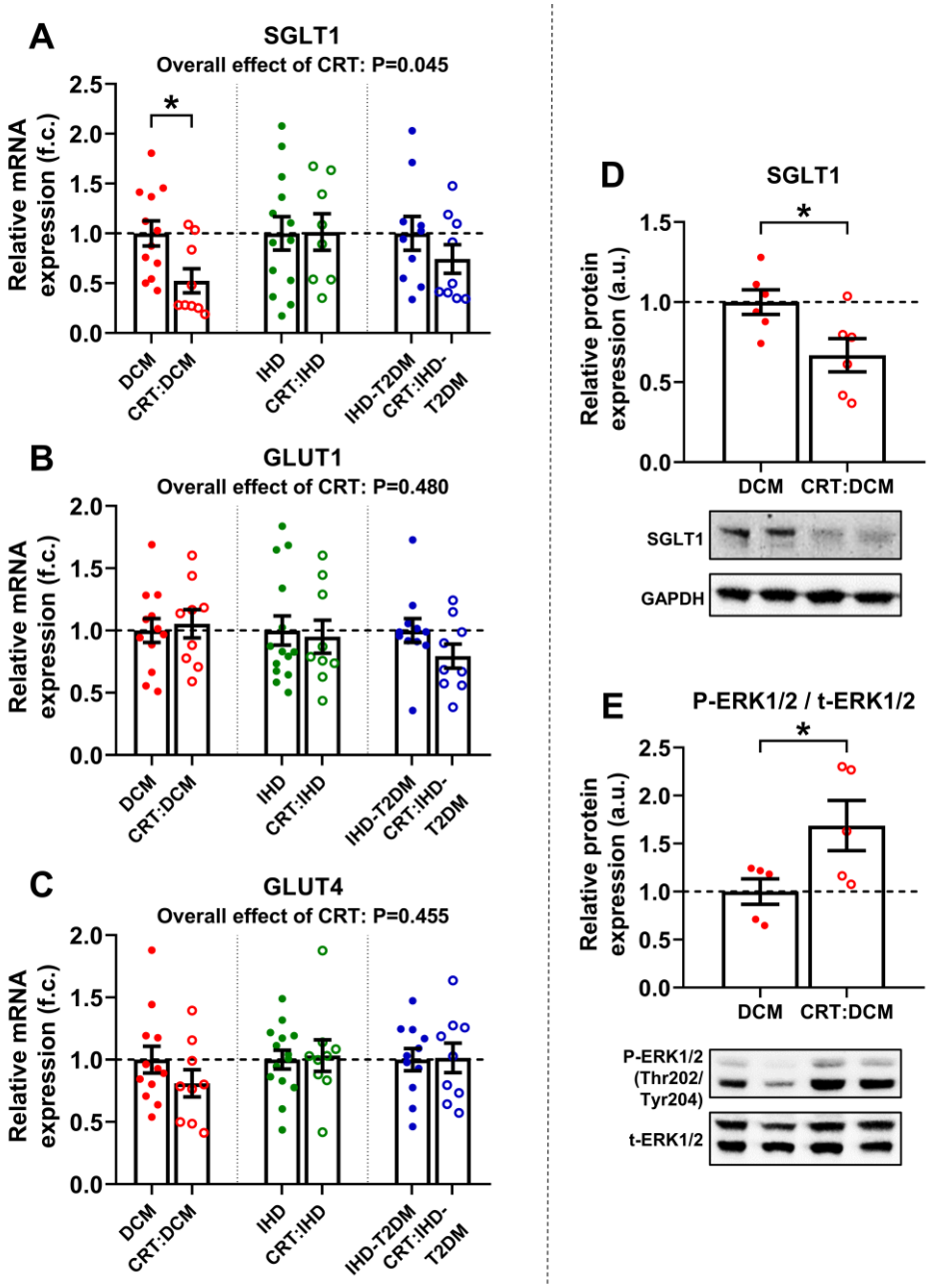

Figure 6. Effect of CRT on LV mRNA expressions of glucose transporters, protein expression of SGLT1, and phosphorylation of ERK1/2

A–C: *Comparison of LV relative mRNA expression of SGLT1, GLUT1, and GLUT4 between HF patients with and without CRT.*
D–E: *Relative protein expressions of LV SGLT1 and phosphorylated ERK1/2 (P–ERK1/2) versus total ERK1/2 (t–ERK1/2) in patients with DCM with and without CRT.*

a.u.: arbitrary units; CRT: cardiac resynchronization therapy; DCM: dilated cardiomyopathy; f. c.: fold change; ERK1/2: extracellular signal–regulated kinase 1/2; GAPDH: glyceraldehyde–3–phosphate dehydrogenase; GLUT1/4: glucose transporter type 1/ 4; HCM: hypertrophic cardiomyopathy; HF: heart failure; LV: left ventricular; IHD: ischemic heart disease; IHD–T2DM: IHD and type 2 diabetes mellitus; SGLT1: sodium–glucose cotransporter 1

4.2. Study in rats with severe HF

4.2.1. Hemodynamic overload–induced LV structural and functional alterations in rats

Post–mortem organ weight measurements confirmed significantly bigger hearts in both pressure (TAC) and volume (ACF) overload–induced HF models compared with respective sham–operated controls both in absolute and indexed (to tibial length) terms (all P<0.001) (Table 3). In both models, LV backward failure was evidenced by absolute and indexed increases in lung weights (all P<0.001) (Table 3). We observed a slightly lower body weight and tibial length in TAC rats compared with Sham–T rats at the end of follow–up, which might represent cardiac cachexia (Table 3). This was not seen in rats with volume overload–induced HF (Table 3).

Table 3. Post–mortem morphometric analyses of rats with heart failure and respective sham–operated controls at the end of follow–up

ACF: aortocaval fistula; TAC: transverse aortic constriction

	Sham–T (n=12, week 14)	**TAC (n=12, week 14)**	***P value***	**Sham–A (n=12, week 24)**	**ACF (n=12, week 24)**	***P value***
Body weight (g)	520 ± 17	439 ± 17	0.002	642 ± 16	702 ± 22	0.042
Tibial length (cm)	4.39 ± 0.04	4.21 ± 0.04	0.005	4.63 ± 0.03	4.67 ± 0.05	0.51
Heart weight (g)	1.32 ± 0.05	2.72 ± 0.14	<0.001	1.56 ± 0.04	3.41 ± 0.18	<0.001
Heart weight/ tibial length (g/cm)	0.30 ± 0.01	0.65 ± 0.03	<0.001	0.34 ± 0.01	0.73 ± 0.04	<0.001
Lung weight (g)	1.94 ± 0.07	4.06 ± 0.33	<0.001	2.06 ± 0.08	3.25 ± 0.18	<0.001
Lung weight/ tibial length (g/cm)	0.44 ± 0.01	0.97 ± 0.08	<0.001	0.44 ± 0.02	0.70 ± 0.04	<0.001

continuous variables: mean±SEM

Chronic pressure (TAC model) and volume (ACF model) overload, respectively, resulted in severe LV hypertrophy compared with respective controls, as indicated by the gradual increase in LV mass detected with serial echocardiography (P_{TAC}<0.001 and P_{ACF}<0.001) (Figures 7A and 8A). Representative LV sections at the midpapillary level show concentric hypertrophy in rats with TAC, and eccentric hypertrophy in rats with ACF, as compared with healthy controls (Figures 7B and 8B).

In rats with chronic pressure overload–induced HF, LVESP was significantly higher compared with controls (234±11 mmHg vs. 121±5 mmHg, P<0.001) at the end of follow–up (Figure 7C). This suggests that the operative model successfully evoked pressure overload. There was evidence of moderate LV dilation in TAC hearts as per LVEDD values (9.0±0.2 mm vs. 7.6±0.2 mm, P<0.001), whereas LV systolic function was severely compromised, as shown by significantly lower LV EF values at the end of the experimental period (P<0.001) (Figure 7D). In contrast, LV contractility (ESPVR) was preserved at the end of the follow–up (Figure 7D), whereas Tau was significantly prolonged in TAC animals (Figure 7D). The pathological nature of LV hypertrophy in TAC was evidenced by the several–fold increase in LV mRNA expression ratio of β/α–MHC (Figure 7E). Furthermore, the LV mRNA expression of Col1a1 showed a significant upregulation (P=0.040) with several–fold increase in expressions of the profibrotic regulators CTGF and TGF–β, respectively (both P<0.001) (Figure 7E).

In rats with chronic volume overload–induced HF, at the end of the follow–up, LVEDD was significantly higher in ACF rats versus controls (13.4±0.4 mm vs. 8.4±0.2 mm, P<0.001) (Figure 8C). This indicates substantial LV dilation in this model, suggesting the successful induction of chronic volume overload. In these ACF rats, EF showed a moderate, but significant reduction, indicating systolic dysfunction compared with sham controls (P=0.046) (Figure 8D). However, LV contractility was severely compromised according to ESPVR values (P<0.001), which marker is less dependent on preload (Figure 8D) in contrast to LV EF. Severe LV diastolic dysfunction was evidenced by the significant prolongation of Tau (P=0.009) (Figure 8D). Compared with Sham–A controls, the several fold increase in the LV mRNA expression ratio of β/α–MHC (P<0.001) reinforced the pathological nature of LV hypertrophy in ACF, as did the significant increase in the mRNA expressions fibrotic markers Col1a1 (P=0.028), CTGF (P<0.001), and TGF–β (P=0.002), respectively, (Figure 8E).

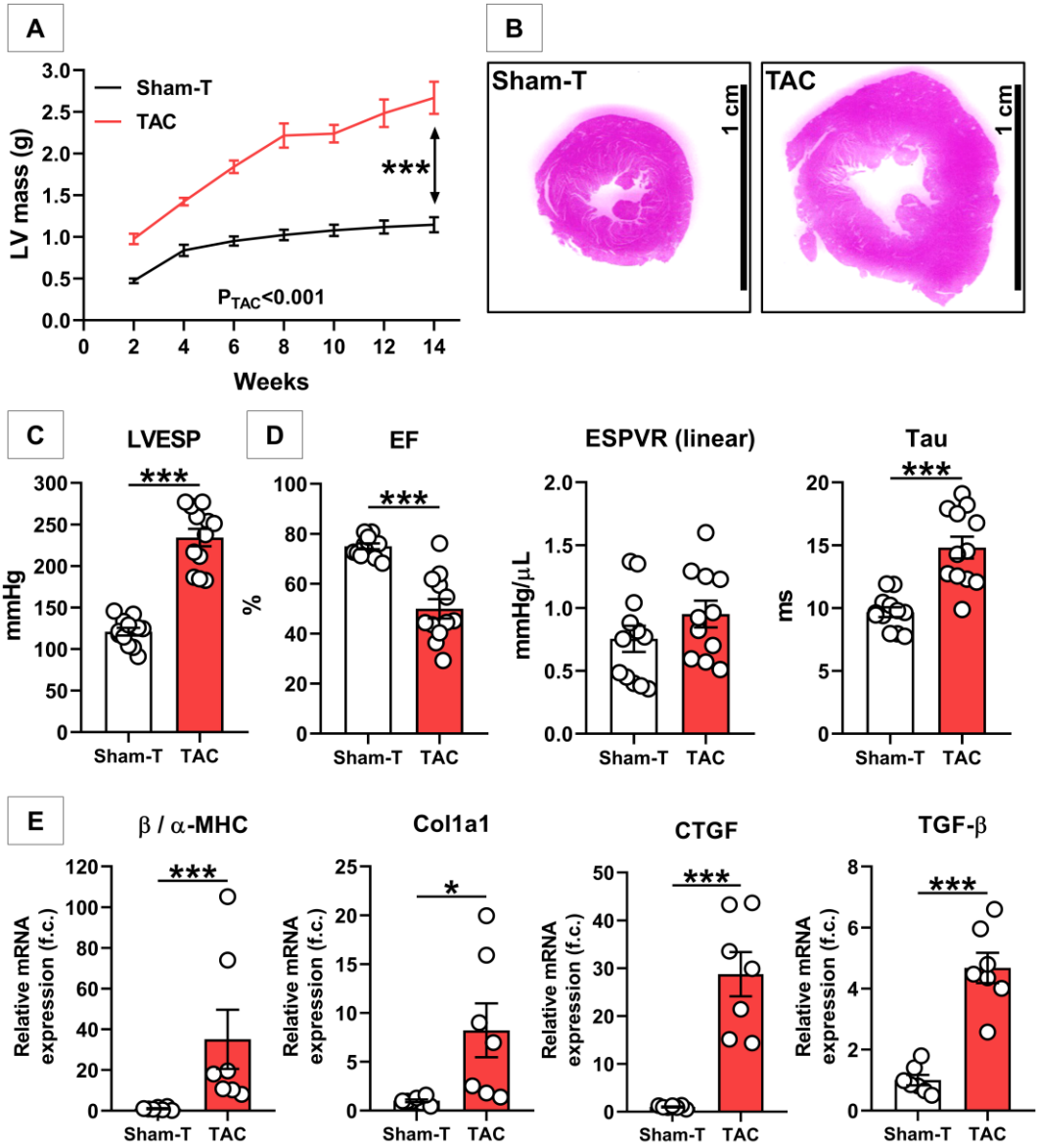

Figure 7. Characterization of pressure overload–induced HF in rats

A: *Temporal changes in LV mass according to the control (Sham–T) and TAC groups.*
B: *Representative histological section at the mid–papillary level of a control (Sham–T) and a TAC heart.*
C–D: *LV functional parameters (LVESP, EF, ESPVR, and Tau) in Sham–T and TAC groups.*
E: *LV myocardial mRNA expressions of markers of pathological hypertrophy (β/α–MHC ratio) and fibrosis (Col1a1, CTGF, TGF–β) in control and TAC hearts.*

β/α–MHC: β/α–myosin heavy chain; Col1a1: collagen type I alpha 1; CTGF: connective tissue growth factor; EF: ejection fraction; ESPVR: end-systolic pressure-volume relationship; f.c.: fold change; LV: left ventricular; LVESP: left ventricular end-systolic pressure; TAC: transverse aortic constriction; TGF–β: transforming growth factor beta

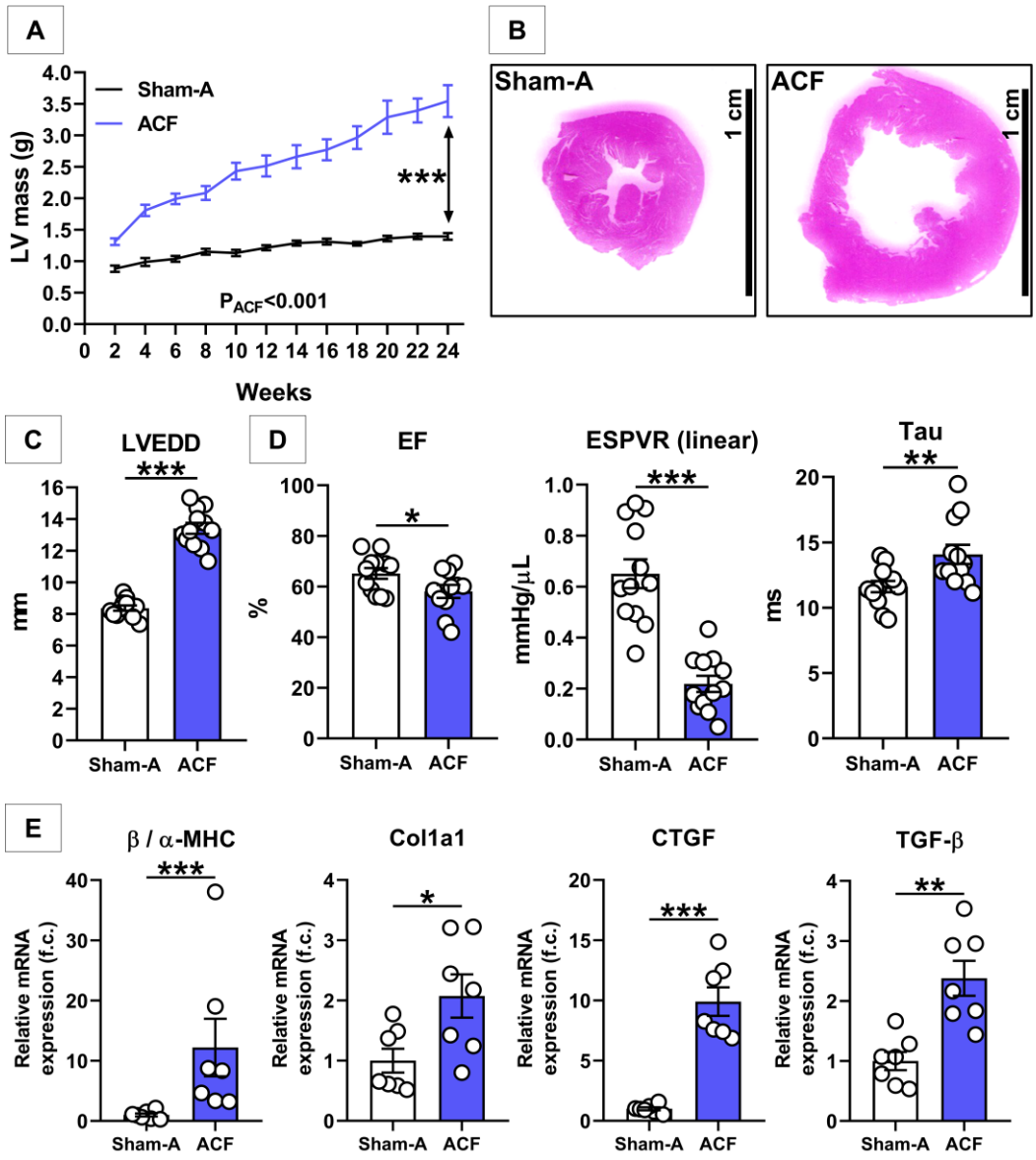

Figure 8. Characterization of volume overload–induced HF in rats

A: *Temporal changes in LV mass according to the control (Sham–A) and ACF groups.*
B: *Representative histological section at the mid–papillary level of a control (Sham–A) and an ACF heart.*
C–D: *LV structural and functional parameters (LVEDD, EF, ESPVR, and Tau) in Sham–A and ACF groups.*
E: *LV myocardial mRNA expressions of markers of pathological hypertrophy (β/α–MHC ratio) and fibrosis (Col1a1, CTGF, TGF–β) in control and ACF hearts.*

β/α–MHC: β/α–myosin heavy chain; ACF: aortocaval fistula; Col1a1: collagen type I alpha 1; CTGF: connective tissue growth factor; EF: ejection fraction; ESPVR: end-systolic pressure-volume relationship; f.c.: fold change; LV: left ventricular; LVESP: left ventricular end-systolic pressure; TGF–β: transforming growth factor beta

4.2.2. Changes in LV protein expression in the two HF models

In rats with pressure overload–induced HF (TAC), LV SGLT1 protein expression was significantly upregulated as compared with controls ($P<0.001$) (Figure 9A). This corresponded to an average of ~1.7–fold increase in LV SGLT1 expression. In these hearts, the reactive oxygen species (ROS)–producing Nox4 protein expression showed a similar upregulation ($P=0.004$) (Figure 9B). As for possible mediators of changes in SGLT1 expression, the activating phosphorylation of ERK1/2 was similar between TAC and control animals (Figure 9C), whereas that of AMPKα tended to be lower in TAC ($P=0.16$) (Figure 9D). However, phosphorylation of ACC at the AMPK–specific Ser79 residue was significantly downregulated in TAC as compared with controls ($P=0.011$) (Figure 9E), suggesting compromised AMPKα activity. Blots are depicted in Figures 9F–J.

Chronic volume overload (ACF) was associated with significant upregulation of LV SGLT1 protein expression compared with controls ($P=0.008$) (Figure 10A). In extent, this was comparable to that seen in TAC hearts, with an average of ~1.6–fold increase. Similarly, the protein expression of Nox4 was highly upregulated ($P=0.002$) (Figure 10B) in volume overload–induced failing hearts as compared with controls. Unlike in TAC, however, ACF rats presented with a significantly decreased activating phosphorylation of the survival kinase ERK1/2 ($P=0.003$) (Figure 10C), while that of AMPKα was preserved (Figure 10D). Nonetheless, phosphorylation of ACC at the AMPK–specific site was significantly decreased compared to Sham–A controls ($P=0.041$) (Figure 10E), similarly to TAC hearts. Blots are depicted in Figures 10F–J.

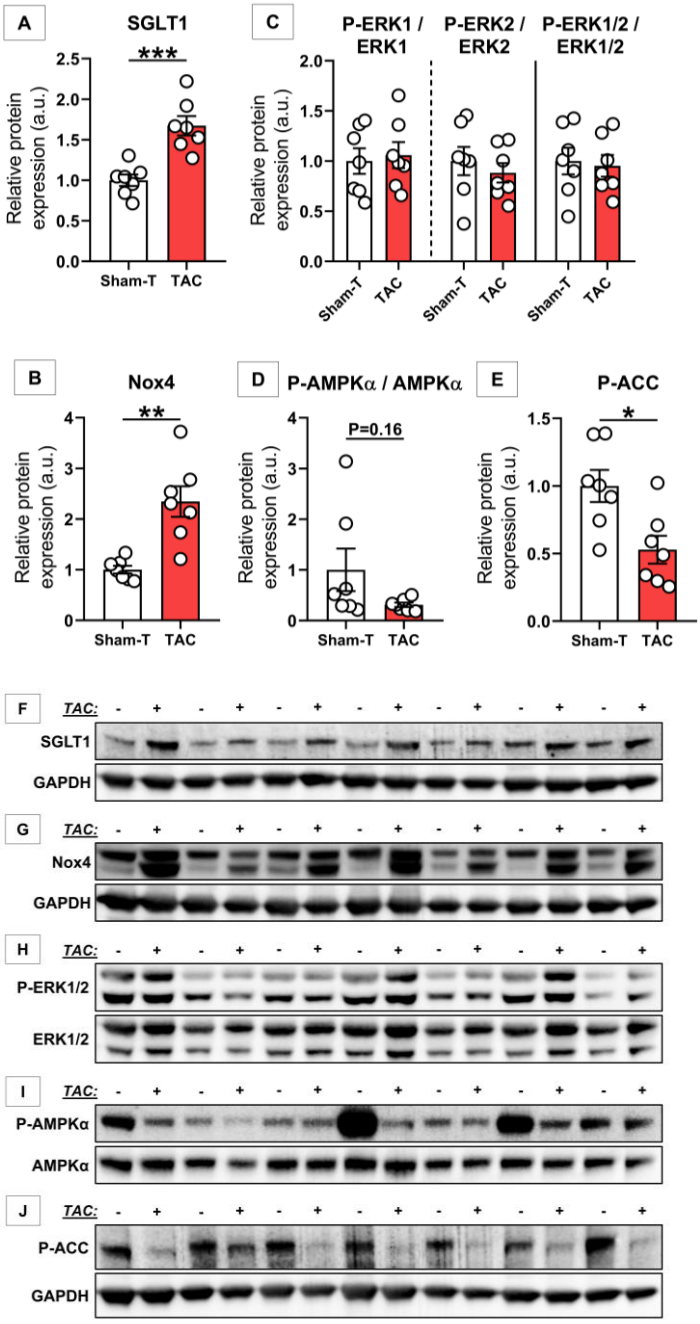

Figure 9. Western blot analysis of left ventricular myocardial samples from controls and rats with pressure overload–induced HF

A–E*: Relative protein expression of left ventricular SGLT1, Nox4, phosphorylated ERK1/2 (P–ERK1/2; Thr202/Tyr204) and total ERK1/2 ratios, phosphorylated AMPKα (P–AMPKα; Thr172) and total AMPKα ratios; and phosphorylated ACC (P–ACC; Ser79).*
F–J*: Cropped full–length blots according to the quantification.*

ACC: acetyl coenzyme–A carboxylase; AMPKα: adenosine monophosphate–activated protein kinase α catalytic subunit; a.u.: arbitrary units; ERK1/2: extracellular signal–regulated protein kinase 1/2; GAPDH: glyceraldehyde–3–phosphate dehydrogenase; Nox4: nicotinamide adenine dinucleotide phosphate (NADPH) oxidase 4; SGLT1: sodium–glucose cotransporter 1; TAC: transverse–aortic constriction

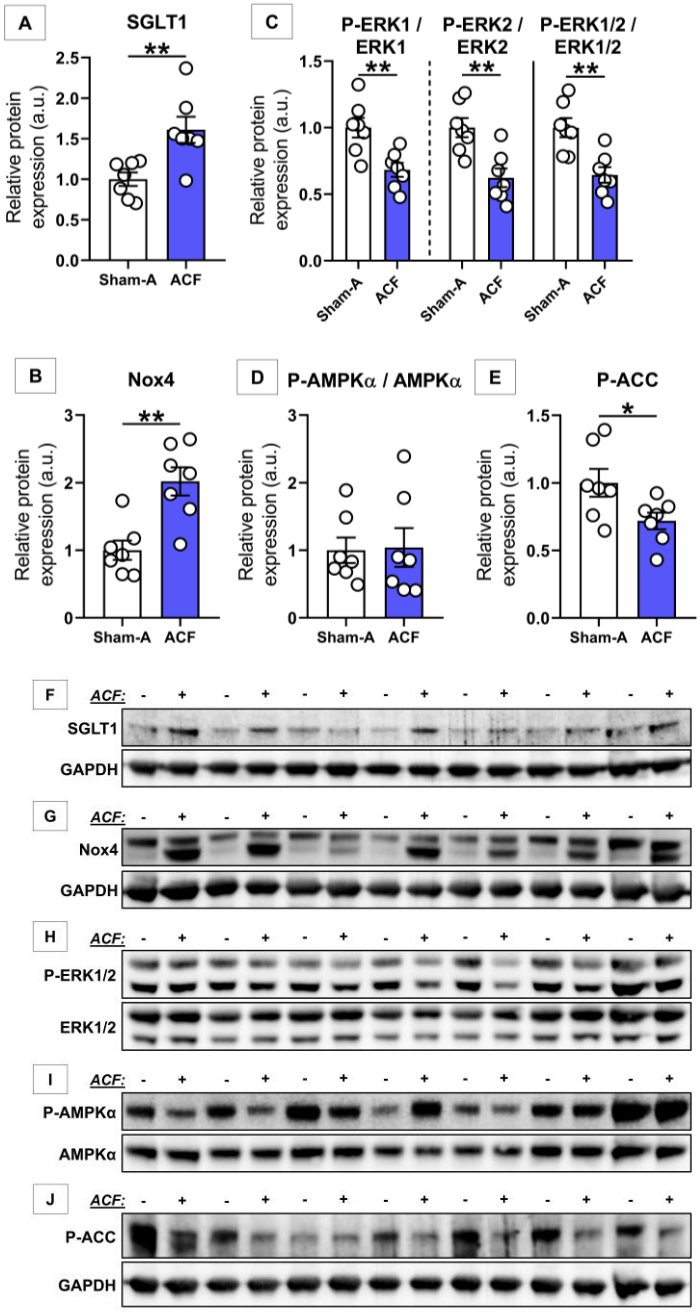

Figure 10. Western blot analysis of left ventricular myocardial samples from rats with sham operation and volume overload–induced heart failure.

***A–E**: Relative protein expression of left ventricular SGLT1, Nox4, phosphorylated ERK1/2 (P–ERK1/2; Thr202/Tyr204) and total ERK1/2 ratios, phosphorylated AMPKα (P–AMPKα; Thr172) and total AMPKα ratios; and phosphorylated ACC (P–ACC; Ser79).*
***F–J**: Cropped full–length blots according to the quantification.*

ACC: acetyl coenzyme–A carboxylase; ACF: aortocaval fistula; AMPKα: adenosine monophosphate–activated protein kinase α catalytic subunit; a.u.: arbitrary units; ERK1/2: extracellular signal–regulated protein kinase 1/2; GAPDH: glyceraldehyde–3–phosphate dehydrogenase; Nox4: nicotinamide adenine dinucleotide phosphate (NADPH) oxidase 4; SGLT1: sodium–glucose cotransporter 1

4.2.3. Correlation between left ventricular SGLT1 expression and the extent of myocardial nitro–oxidative stress

Figure 11A shows the representative hematoxylin–eosin–stained LV sections from Sham–T, TAC, Sham–A, and ACF rat hearts, respectively. Immunohistochemical staining against the nitro–oxidative stress markers 3–nitrotyrosin (3–NT) and 4–hydroxy–nonenal (4–HNE) revealed a higher positivity in the failing hearts compared with respective controls (as assessed by the intensity of positively stained tissue versus total tissue area) (Figure 11B–C), indicating increased nitro–oxidative stress in failing rats hearts.

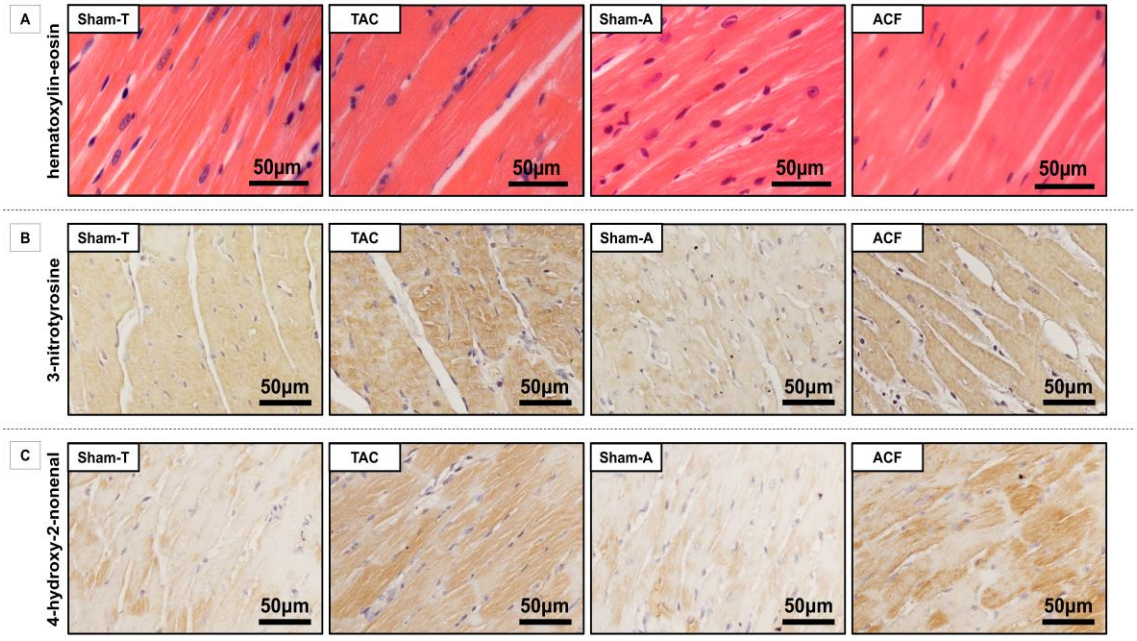

Figure 11. Histological sections from sham–operated and hemodynamically–overloaded failing rat hearts

***A**: Representative left ventricular sections of Sham–T, TAC, Sham–A, and ACF hearts stained with hematoxylin–eosin.*
***B-C**: Representative left ventricular sections of Sham–T, TAC, Sham–A, and ACF hearts with immunohistochemical staining against the nitrosative stress marker 3–nitrotyrosine, and the oxidative stress 4–hydroxy–2–nonenal. Hematoxylin was used to stain nuclei. Images were captured with 20x objective, scale bars are shown for reference on each representative section.*

ACF: aortocaval fistula; TAC: transverse aortic constriction

In the Sham–T and TAC groups, LV SGLT1 protein expression showed a significant correlation with the ROS–generating Nox4 protein expression (r_s=0.855, P<0.001) (Figure 12A). This was also the case with Sham–A and ACF rats (r_s=0.798, P=0.001) (Figure 12B). In rats with pressure and volume overload–induced HF, LV SGLT1 protein expression significantly correlated with the extent of myocardial 3–NT positivity (TAC & ACF: r_s=0.818, P=0.006) (Figure 12C) and that of 4–HNE positivity (TAC & ACF: r_s=0.733, P=0.020) (Figure 12D), indicating a robust association between LV SGLT1 protein expression and the level of nitro–oxidative stress in failing hearts.

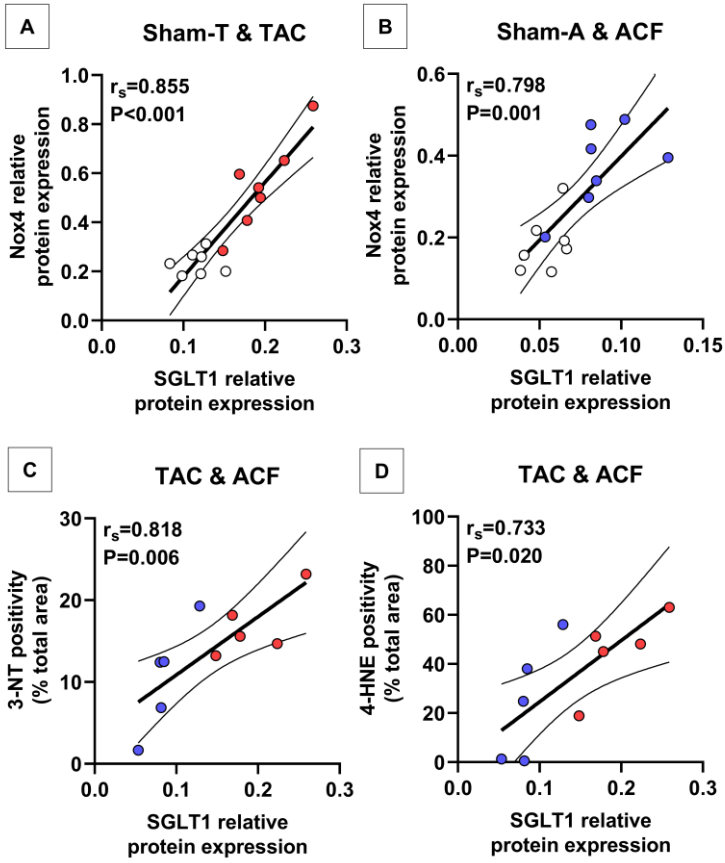

Figure 12. *Correlation between left ventricular SGLT1 protein expression, Nox4 protein expression and the extent of myocardial nitro–oxidative stress*

A–B: *Correlation analysis of left ventricular SGLT1 and Nox4 protein expression in the Sham–T and TAC, and Sham–A and ACF groups, respectively.*
C-D: *Correlation analysis of western blot–derived myoxardial left ventricular SGLT1 protein expression and immunohistochemical analysis-derived 3–NT positivity and 4-HNE (expressed as percentage of the total area), respectively, in rats with HF (TAC and ACF).*

3-NT: 3-nitrotyrosine; 4-HNE: 4–hydroxy–2–nonenal; ACF: aortocaval fistula; TAC: transverse aortic constriction

5. Discussion

The class of SGLT2 inhibitors – originally designed as glucose–lowering medications – has become an essential class of agents in therapy of patients with HF, as current clinical guidelines on the treatment of HF now recommend these medications as baseline therapy irrespective of diabetic status (31). Despite the rapidly growing number of patients using these medications, the exact mechanism of action resulting in salutary cardiovascular effects are unclear. It is now widely accepted that SGLT2 inhibitors – at least in part – exert direct cardiovascular effects. However, the primary pharmacological target of SGLT2 inhibitors (i.e. SGLT2) is not convincingly expressed in the heart, whereas SGLT1, the other major glucose transporter targeted non–specifically by SGLT2 inhibitors, is highly expressed. In the present studies, we sought to investigate whether LV SGLT1 expression is altered in HF compared with non–failing controls, and whether its expression correlates with clinical and pathophysiological parameters in humans and rats with severe HF.

5.1. Expression of SGLT1 in cardiac tissue

Previous studies showed that SGLT1 is most abundantly expressed in the small intestine, but is also highly expressed in the heart of human and murine alike (46, 58, 64), being co–localized with the cardiomyocyte membrane marker Na–K–ATPase (49, 66). However, some studies reported that cultured coronary endothelial cells and capillaries of rat hearts also express significant levels of SGLT1 (62). Vrhovac and colleagues (69) further postulated that SGLT1 expression in the heart is exclusively confined to the microvasculature, as it co–localizes with aquaporin–1 (marker of capillary walls), and not the cardiomyocyte membrane marker Na–K–ATPase. In the present study using microscopic immunohistochemical analysis, we found that SGLT1 expression is prominent in cardiomyocytes of human failing hearts. Indeed, staining for SGLT1 returned a highly positive signal predominantly in regions of cardiomyocytes, whereas intensity was considerably lower in areas of fibrotic or adipose tissues. Nonetheless, staining of an epicardial vessel in a patient with DCM demonstrates that the vessel wall, especially the layers of endothelial and smooth muscle cells are also positive for SGLT1. According to our immunofluorescent data, we found that myocardial SGLT1 co–localized with Na–K–ATPase, in line with previous studies in

human hearts (49). Therefore, it is reasonable to assume that the majority of SGLT1 expression in the heart is related to cardiomyocytes, while the vasculature also expresses SGLT1.

5.2. Changes in myocardial SGLT1 expression in HF

Leveraging the Heart Transplantation Biobank of the Heart and Vascular Center, Semmelweis University, we analyzed myocardial SGLT1 expression in LV samples originating from failing and non–failing human hearts. On a relatively large number of samples, we demonstrate that patients with end–stage HF related to DCM or IHD have a significantly higher myocardial SGLT1 expression as compared with non–failing controls, in line with previous studies (49, 67). This increase was found to be largely independent of age, sex, and BMI. Importantly, the presence of T2DM itself did not further alter the level of upregulation of myocardial SGLT1 in HF, which was also observed in prior reports (58, 67). Interestingly, LV SGLT1 expression was not increased in patients with HCM in our study. Persons with end–stage HF due to HCM were much younger, had better LV EF, and non–dilated LV by virtue of their unique myocardial pathology, unlike patients with DCM or IHD, which might partially explain the differences in SGLT1 expression. Interestingly, Di Franco et al. (49) found a modest but significant increase in LV SGLT1 protein expression in patients with HCM compared with non–failing controls, but LV septal samples were obtained during myectomy in their study, suggesting that those patients were in a different HF phase, unlike ours. Finally, two previous studies reported no significant increase in LV SGLT1 expression in patients with DCM compared with non–failing controls (32, 58). While the clinical characteristics of those patients in the two studies are scarcely defined, it is unknown how many of those were on CRT. We found that CRT was associated with a significantly lower LV SGLT1 expression in patients with DCM, which might account for the differences between our results and those of the two previous studies. In fact, we showed that ACF rats that have severely dilated LV similar to patients with DCM also show a significant upregulation of LV SGLT1 protein expression. This was also the case in rats with chronic pressure overload–induced HF (TAC), as well, in line with a previous study using a similar model (71). Therefore, in murine models and in patients

with HF, upregulation of myocardial SGLT1 might be a common hallmark in HF despite varying etiologies.

5.3. Possible mediators of LV SGLT1 expression in HF

Data are scarce regarding the possible mediators that regulate LV SGLT1 expression in HF. In a mouse model of myocardial ischemia–reperfusion injury, AMPK was found to be responsible for upregulating SGLT1 (68). In a genetic model of HF in mice, overactivation of AMPK results in substantial upregulation of myocardial SGLT1 (66, 79). In humans with HF, a previous study identified that in patients with HCM or IHD, SGLT1 expression increased in conjunction with the activating phosphorylation of AMPK (49). On the contrary, in the present study on relatively high number of human LV samples, we found that activating phosphorylation of AMPK was numerically, but not significantly (except in patients with IHD and T2DM) increased in HF samples compared with non–failing controls. Several medications are known to increase AMPK activity in the heart, especially the antidiabetic agent metformin (88), which might account for the higher level of AMPK activity in patients with T2DM (many of whom were on metformin, a potent AMPK activator in the heart). However, in two distinct types of small–animal HF models, we found that AMPK activation (based on the phosphorylation of its target ACC) was significantly lower as compared with non–failing controls. This is in line with previous studies documenting compromised AMPK activity in the failing heart (89, 90).

In a model of acute myocardial ischemia–reperfusion injury, ERK1/2 was implicated as a positive regulator of SGLT1, similarly to AMPK (68). Furthermore, the activating phosphorylation of ERK1/2 was found to be upregulated along with that of AMPK in failing human LV samples, as SGLT1 expression was also increased (49). In our present studies, we documented that in humans with end–stage HF (except in HCM) and in rats with chronic volume–overload induced HF, ERK1/2 activity was significantly compromised. This is in agreement with studies in humans, demonstrating that end–stage HF was coupled with substantial decrease in ERK1/2 phosphorylation compared to non–failing controls (91). On the contrary, ERK1/2 activity was not significantly reduced in patients with HCM and in rats with chronic pressure overload–induced HF, both conditions are characterized by massive hypertrophy of the LV with relatively less

dilation as compared with DCM patients and the rat model of chronic volume overload–induced HF. The differences we found regarding ERK1/2 activity between HF with predominant LV dilation versus HF without significant LV dilation is in good agreement with previous studies, reflecting temporal molecular differences between these two distinct pathological phenotypes of LV failure. Specifically, there is evidence that myocardial ERK1/2 is initially increased in response to pressure overload, and gradually declines as decompensation develops, reaching the level of controls and beyond (71, 92, 93). Furthermore, suppression of myocardial ERK1/2 activity predisposes the LV to dilation rather than concentric hypertrophy (94). Therefore, in our study, preserved ERK1/2 activity along with non–substantial LV dilation in patients with HCM and in rats with chronic pressure overload–induced HF might reflect diminishing ERK1/2 activity.

Taken together, while AMPK might play a role in upregulation of myocardial SGLT1 during ischemia–reperfusion injury and development of a special type of genetic cardiomyopathy (related to constant AMPK overactivation), we found that LV SGLT1 expression was upregulated despite reduction in the activating phosphorylation of LV AMPK in two distinct preclinical HF models. Therefore, AMPK might play some role in regulating the expression of myocardial SGLT1, but it might not be a prerequisite for upregulation of SGLT1.

On the contrary, our human study clearly indicated that reduction in the activating phosphorylation of the survival kinase ERK1/2 concurs with upregulation of SGLT1. We observed these opposing changes also in two distinct small animal models of chronic HF. Such counter–regulation in SGLT1 expression and ERK1/2 activating phosphorylation was documented previously in cultured rabbit renal proximal tubule cells, in which activation of ERK1/2 resulted in suppressed expression of SGLT1 expression (95, 96). Furthermore, in mice with global SGLT1 knockout, myocardial ERK1/2 activity was increased under basal conditions and exhibited a significantly higher increment in response to early pressure overload than in wildtype littermates (71). These might indicate that reduced ERK1/2 activity might be related to increase in SGLT1 expression, and vice versa, restoration of ERK1/2 survival kinase activity might downregulate SGLT1. Indeed, in patients with CRT, we observed a significantly reduced LV SGLT1 expression as compared with non–CRT failing hearts. This was

accompanied by converse upregulation in the activating phosphorylation of ERK1/2. Further studies are needed to elucidate this possible inverse connection between myocardial SGLT1 and the activity of the survival kinase ERK1/2.

5.4. Putative pathophysiological and clinical relevance of changes in myocardial SGLT1 expression

The question remains: is increase in myocardial SGLT1 expression pathophysiologically and clinically relevant?

In our study, LV SGLT1 expression significantly correlated with the severity of HF in humans. Specifically, SGLT1 mRNA and protein expression gradually increased with the severity of LV dilation and systolic dysfunction. Furthermore, the expression of SGLT1 appeared to be robustly associated with these parameters independent of age, sex, and BMI. Therefore, myocardial SGLT1 might be a novel myocardial tissue marker of LV dilation and systolic dysfunction in HF. Notably, the expression of the other two major glucose transporters (GLUT1 and GLUT4) showed no relevant association with the severity of HF in our study. In the study of Ramratnam and colleagues (79), cardiomyocyte–specific overexpression of SGLT1 in mice for 10 weeks was sufficient to induce LV dilation and dysfunction, as compared with wild–type controls. On the contrary, when SGLT1 expression was suppressed after this period, LV structure and function gradually normalized (79). Indeed, murine hearts subjected to chronic pressure overload are protected from developing HF when SGLT1 is knocked out (71). Therefore, SGLT1 might play a causal role in development and worsening of HF as its forced upregulation results in HF, whereas its suppression prevents HF in response to pathological stimuli.

A previous study showed that SGLT1 plays a role in activating NADPH oxidase–dependent nitro–oxidative stress in cardiomyocytes subjected to high–glucose medium (82). In mice with T2DM presenting with upregulation of myocardial SGLT1, knock down of the transporter was associated with reduced nitro–oxidative stress and inflammation (73). Importantly, in non–diabetic mice, cardiomyocyte–specific knock down of SGLT1 reduced myocardial infarct size in response to ischemia–reperfusion possibly by blunting nitro–oxidative stress (68). In line with these, we show in two pathophysiologically distinct non–diabetic HF models that upregulation of myocardial

SGLT1 is concomitant with the upregulation of NADPH oxidase 4 (Nox4), and correlates with increased myocardial nitro–oxidative stress. All these together suggest that increased SGLT1 expression might play a causal role in the propagation of myocardial nitro–oxidative stress, which might explain how upregulation of SGLT1 is associated with more severe forms of HF in humans. Interestingly, the study of Lambert et al. (67) showed that myocardial SGLT1 upregulation in HF also resulted in heightened intracellular sodium ion overload, as this membrane transporter brings two sodium ions into the cell alongside one glucose molecule. Intracellular sodium ion overload is a common hallmark of failing cardiomyocytes (97). Finally, some studies suggest an important role of SGLT1 in cardiac fibroblasts, as its increased expression resulted in activation of profibrotic signaling and collagen release (63, 75). Indeed, SGLT1 knock down in rats with T2DM reduced interstitial fibrosis in the heart (75). We have shown that profibrotic signaling is significantly upregulated in rats with volume or pressure overload induced HF, in line with increased SGLT1 expression. These profibrotic mechanisms can add to the pathophysiological relevance of SGLT1 in HF. The synthesis of all these pathways is summarized in Figure 13.

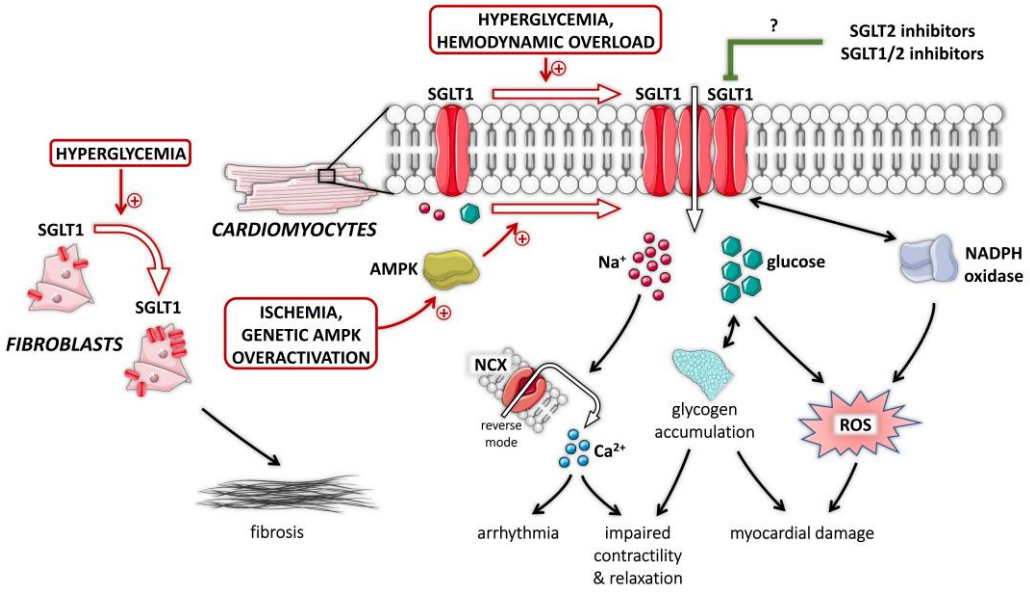

Figure 13. The putative role of SGLT1 in myocardial pathophysiological processes

AMPK: adenosine monophosphate–activated protein kinase; NADPH: nicotinamide adenine dinucleotide phosphate; NCX: Na^+/Ca^{2+} exchanger; ROS: reactive oxygen species; SGLT1/2: sodium–glucose cotransporter 1/2

Our results have been corroborated by two studies. On the pathophysiological level, Kondo et al. (98) found that in atrial samples from mostly non–diabetic patients with IHD, higher SGLT1 expression was associated with increased NADPH oxidase–related ROS production (98). In these myocardial samples, NADPH oxidase activation and subsequent oxidative damage was suppressed by the least selective SGLT2 inhibitor canagliflozin (which has a clinically relevant SGLT1 blocking effect), and this effect seemed to be dependent on SGLT1 (98). On the clinical level, Täger et al. performed a network meta–analysis of dedicated HF studies and calculated that the efficacy of SGLT2 inhibitor therapy increases in conjunction with the prominence of SGLT1 inhibitory effect of the given agent (99). In other words, non–selective SGLT2 inhibitors with relevant SGLT1 inhibitory effect produce measurably greater clinical benefit in patients with HF by reducing adverse HF–related events, as compared with selective SGLT2 inhibitors.

Taken together, the totality of evidence points toward the direct pathophysiological role of myocardial SGLT1 in developing and worsening HF, its pharmacological blockade reduces nitro–oxidative stress and produces measurable clinical benefit in patients with HF. Therefore, increase in myocardial expression of SGLT1 seems to be pathophysiologically and clinically relevant.

6. Conclusions

In the present studies, we found that LV SGLT1 expression is significantly upregulated in patients with end–stage HF and in two distinct small animal models of severe HF. In fact, SGLT1 is abundant in cardiomyocytes, mainly in the sarcolemma, therefore, it is unlikely that a significant intracellular pool contributes to increased SGLT1 expression in failing hearts. Higher LV SGLT1 expression positively correlates with LV dilation and systolic dysfunction in human hearts. Such increased expression of LV SGLT1 correlates with the extent of myocardial nitro–oxidative stress in failing rat hearts.

In context of previous studies, our results might indicate that SGLT1 is a myocardial tissue marker of LV dilation and systolic dysfunction. Given the fact that SGLT2 inhibitors non–specifically block SGLT1, such increased expression of SGLT1 in failing hearts might be clinically relevant. This might be reinforced by findings of a recent meta–analysis of dedicated HF trials, which suggests that SGLT2 inhibitors with more pronounced SGLT1 inhibitory effects result in significantly better clinical outcomes as compared with highly specific agents. The absence of myocardial SGLT2 expression in human hearts might further underline the possible mediator role of myocardial SGLT1 inhibition by these agents. Furthermore, it might also serve as an explanation as to why deficient SGLT1 activity substantially reduces the risk of HF, whereas patients with deficient SGLT2 activity derive no meaningful benefit compared with unaffected controls.

Overall, myocardial SGLT1 might play an important pathophysiological role in HF and might partially explain the salutary cardiovascular effects of SGLT2 inhibitors, which needs to be further validated.

7. Summary

The rapid success of the antidiabetic agents, SGLT2 inhibitors, in medical treatment of HF regardless of T2DM led to speculations regarding the mechanisms of cardiovascular benefit. Given that genetically reduced functional capacity of SGLT1 – but not that of SGLT2 – is associated with lower risk of HF and mortality, non–specific inhibition of SGLT1 by SGLT2 inhibitors has come under spotlight. Furthermore, a recent meta–analysis found that SGLT2 inhibitors with more pronounced inhibitory effect on SGLT1 produce measurably greater clinical benefits in patients with HF, compared with highly selective agents. These highlight the relevance of quantification of myocardial SGLT1 expression and its pathophysiological role in HF.

Leveraging the Transplantation Biobank of the Heart and Vascular Center, we demonstrated on a relatively high number of LV samples that SGLT1 – but not SGLT2 – is highly expressed in cardiomyocytes of humans with end–stage HF, as well as in non–failing control hearts. Immunohistochemical analyses revealed that cardiomyocytes are the primary source of SGLT1 expression in the human myocardium, and its primary location is likely the sarcolemma of cardiomyocytes. While the mRNA expressions of GLUT1 and SGLT1 were similarly upregulated in humans with HF (except in HCM) versus controls, the expression of these two glucose transporters showed no correlation. Accordingly, only the expression of SGLT1 correlated significantly with the extent of LV dilation and lower EF, even after adjusting for age, sex, and BMI. The higher expression of SGLT1 in failing hearts was also evident on the protein level. At the same time, we observed a reciprocal downregulation in the activating phosphorylation of the survival kinase ERK1/2.

In two pathophysiologically distinct small animal models of HF, we corroborated our findings in humans by showing a similar upregulation in LV SGLT1 protein expression as compared with healthy controls. The expression of SGLT1 showed robust correlation with that of the ROS–generating Nox4, and hence higher SGLT1 expression was associated with increased nitro–oxidative stress in these failing rat hearts. Similar to humans, our rodent studies suggest that the survival kinase ERK1/2 might be a negative regulator of myocardial SGLT1 expression.

7. Összefoglaló

Az antidiabetikus SGLT2 inhibitorok gyors sikert arattak a szívelégtelenség (SZE) gyógyszeres terápiájában cukorbetegség jelenlététől függetlenül, melynek hátterében számos hatásmechanizmus felmerült. A genetikai okokból csökkent SGLT1 aktivitással élő emberek esetében számottevően alacsonyabb a SZE kialakulásának a rizikója és az összemortalitás, míg a csökkent SGLT2 aktivitással élő emberek esetében ez nem figyelhető meg. Ebből adódóan reflektorfénybe került az SGLT2 gátlók által aspecifikus módon blokkolt SGLT1 jelentősége. Egy friss meta–analízis szerint azon SGLT2 inhibitorok, melyek nagyobb mértékben gátolják az SGLT1-et, számottevően jobb klinikai kimenetellel kecsegtetnek a szelektív ágensekhez képest SZE betegekben.

A Városmajori Szív– és Érgyógyászati Klinika Transzplantációs Biobankjában tárolt szívmintákat felhasználva nagy elemszámú betegcsoporton bemutattuk, hogy az SGLT1 nagymértékben expresszálódik kontroll és SZE betegek bal kamrai (BK) szívizommintáiban, míg SGLT2 expresszió nem detektálható. Immunhisztokémiai analízisünk szerint a humán miokardiális SGLT1 expresszió döntő részéért a szívizomsejtek felelősek, elsődlegesen a szarkolemmára lokalizálva. Bár az SGLT1 és a GLUT1 mRNS expressziója hasonló növekedést mutatott a SZE betegek BK-i mintáiban (kivéve HCM-ben szenvedő betegek esetében), azok egymással nem mutattak összefüggést. Csak az SGLT1 expresszió korrelált számottevően a BK-i dilatációval és csökkent ejekciós frakcióval (EF), mely életkortól, nemtől, és BMI-től függetlenül fennállt. A magasabb SGLT1 expresszió a SZE szívekben fehérje szinten is igazolható volt. Ezzel egyidőben az ERK1/2 aktivációs foszforilációjának reciprok csökkenését figyeltük meg.

Fenti humán eredményeinket igazoltuk két patofiziológiailag igen eltérő kisállat SZE modellen, melyekben a BK-i SGLT1 expresszió szintén számottevő emelkedést mutatott egészséges kontrollokhoz képest. Az SGLT1 expresszió nagymértékben korrelált az oxigéntartalmú szabad gyököket termelő Nox4 fehérje expressziójával, és így a nagyobb mértékű miokardiális nitro-oxidatív stresszel. Humán eredményeinkhez hasonlóan ezen patkánymodellekben is azt találtuk, hogy a túlélési jelátvitelt aktiváló ERK1/2 szignalizációja gyengül, mely így az SGLT1 expresszió negatív regulátora lehet.

8. References

1. Bozkurt B, Coats AJS, Tsutsui H, Abdelhamid CM, Adamopoulos S, Albert N, Anker SD, Atherton J, Bohm M, Butler J, Drazner MH, Felker GM, Filippatos G, Fiuzat M, Fonarow GC, Gomez-Mesa JE, Heidenreich P, Imamura T, Jankowska EA, Januzzi J, Khazanie P, Kinugawa K, Lam CSP, Matsue Y, Metra M, Ohtani T, Piepoli MF, Ponikowski P, Rosano GMC, Sakata Y, Starling RC, Teerlink JR, Vardeny O, Yamamoto K, Yancy C, Zhang J, Zieroth S. (2021) Universal definition and classification of heart failure: a report of the Heart Failure Society of America, Heart Failure Association of the European Society of Cardiology, Japanese Heart Failure Society and Writing Committee of the Universal Definition of Heart Failure. European Journal of Heart Failure, 23: 352-380.
2. Roberts NLS, Mountjoy-Venning WC, Anjomshoa M, Banoub JAM, Yasin YJ. (2019) GBD 2017 Disease and Injury Incidence and Prevalence Collaborators. Global, regional, and national incidence, prevalence, and years lived with disability for 354 diseases and injuries for 195 countries and territories, 1990-2017: a systematic analysis for the Global Burden of Disease Study. Lancet, 392: 1789-2018.
3. Savarese G, Becher PM, Lund LH, Seferovic P, Rosano GMC, Coats AJS. (2022) Global burden of heart failure: a comprehensive and updated review of epidemiology. Cardiovascular Research, 118: 3272-3287.
4. Virani SS, Alonso A, Aparicio HJ, Benjamin EJ, Bittencourt MS, Callaway CW, Carson AP, Chamberlain AM, Cheng S, Delling FN, Elkind MSV, Evenson KR, Ferguson JF, Gupta DK, Khan SS, Kissela BM, Knutson KL, Lee CD, Lewis TT, Liu J, Loop MS, Lutsey PL, Ma J, Mackey J, Martin SS, Matchar DB, Mussolino ME, Navaneethan SD, Perak AM, Roth GA, Samad Z, Satou GM, Schroeder EB, Shah SH, Shay CM, Stokes A, VanWagner LB, Wang NY, Tsao CW, American Heart Association Council on E, Prevention Statistics C, Stroke Statistics S. (2021) Heart Disease and Stroke Statistics-2021 Update: A Report From the American Heart Association. Circulation, 143: e254-e743.
5. Uthman L, Baartscheer A, Schumacher CA, Fiolet JWT, Kuschma MC, Hollmann MW, Coronel R, Weber NC, Zuurbier CJ. (2018) Direct Cardiac

Actions of Sodium Glucose Cotransporter 2 Inhibitors Target Pathogenic Mechanisms Underlying Heart Failure in Diabetic Patients. Frontiers in Physiology, 9: 1575.

6. Nissen SE, Wolski K. (2007) Effect of rosiglitazone on the risk of myocardial infarction and death from cardiovascular causes. New England Journal of Medicine, 356: 2457-2471.
7. Zelniker TA, Braunwald E. (2020) Mechanisms of Cardiorenal Effects of Sodium-Glucose Cotransporter 2 Inhibitors: JACC State-of-the-Art Review. J Am Coll Cardiol, 75: 422-434.
8. Zinman B, Wanner C, Lachin JM, Fitchett D, Bluhmki E, Hantel S, Mattheus M, Devins T, Johansen OE, Woerle HJ, Broedl UC, Inzucchi SE, Investigators E-RO. (2015) Empagliflozin, Cardiovascular Outcomes, and Mortality in Type 2 Diabetes. N Engl J Med, 373: 2117-2128.
9. Neal B, Perkovic V, Mahaffey KW, de Zeeuw D, Fulcher G, Erondu N, Shaw W, Law G, Desai M, Matthews DR, Group CPC. (2017) Canagliflozin and Cardiovascular and Renal Events in Type 2 Diabetes. N Engl J Med, 377: 644-657.
10. Wiviott SD, Raz I, Bonaca MP, Mosenzon O, Kato ET, Cahn A, Silverman MG, Zelniker TA, Kuder JF, Murphy SA, Bhatt DL, Leiter LA, McGuire DK, Wilding JPH, Ruff CT, Gause-Nilsson IAM, Fredriksson M, Johansson PA, Langkilde AM, Sabatine MS, Investigators D-T. (2019) Dapagliflozin and Cardiovascular Outcomes in Type 2 Diabetes. N Engl J Med, 380: 347-357.
11. Perkovic V, Jardine MJ, Neal B, Bompoint S, Heerspink HJL, Charytan DM, Edwards R, Agarwal R, Bakris G, Bull S, Cannon CP, Capuano G, Chu PL, de Zeeuw D, Greene T, Levin A, Pollock C, Wheeler DC, Yavin Y, Zhang H, Zinman B, Meininger G, Brenner BM, Mahaffey KW, Investigators CT. (2019) Canagliflozin and Renal Outcomes in Type 2 Diabetes and Nephropathy. N Engl J Med, 380: 2295-2306.
12. Cannon CP, Pratley R, Dagogo-Jack S, Mancuso J, Huyck S, Masiukiewicz U, Charbonnel B, Frederich R, Gallo S, Cosentino F, Shih WJ, Gantz I, Terra SG, Cherney DZI, McGuire DK, Investigators VC. (2020) Cardiovascular Outcomes with Ertugliflozin in Type 2 Diabetes. N Engl J Med, 383: 1425-1435.

13. Bhatt DL, Szarek M, Pitt B, Cannon CP, Leiter LA, McGuire DK, Lewis JB, Riddle MC, Inzucchi SE, Kosiborod MN, Cherney DZI, Dwyer JP, Scirica BM, Bailey CJ, Diaz R, Ray KK, Udell JA, Lopes RD, Lapuerta P, Steg PG, Investigators S. (2021) Sotagliflozin in Patients with Diabetes and Chronic Kidney Disease. N Engl J Med, 384: 129-139.
14. Zelniker TA, Braunwald E. (2020) Clinical Benefit of Cardiorenal Effects of Sodium-Glucose Cotransporter 2 Inhibitors: JACC State-of-the-Art Review. J Am Coll Cardiol, 75: 435-447.
15. Packer M. (2023) SGLT2 inhibitors: role in protective reprogramming of cardiac nutrient transport and metabolism. Nat Rev Cardiol, doi:10.1038/s41569-022-00824-4.
16. Kanai Y, Lee WS, You G, Brown D, Hediger MA. (1994) The human kidney low affinity Na+/glucose cotransporter SGLT2. Delineation of the major renal reabsorptive mechanism for D-glucose. J Clin Invest, 93: 397-404.
17. Vallon V, Platt KA, Cunard R, Schroth J, Whaley J, Thomson SC, Koepsell H, Rieg T. (2011) SGLT2 mediates glucose reabsorption in the early proximal tubule. J Am Soc Nephrol, 22: 104-112.
18. Han L, Qu Q, Aydin D, Panova O, Robertson MJ, Xu Y, Dror RO, Skiniotis G, Feng L. (2022) Structure and mechanism of the SGLT family of glucose transporters. Nature, 601: 274-279.
19. Rieg T, Masuda T, Gerasimova M, Mayoux E, Platt K, Powell DR, Thomson SC, Koepsell H, Vallon V. (2014) Increase in SGLT1-mediated transport explains renal glucose reabsorption during genetic and pharmacological SGLT2 inhibition in euglycemia. Am J Physiol Renal Physiol, 306: F188-193.
20. Umino H, Hasegawa K, Minakuchi H, Muraoka H, Kawaguchi T, Kanda T, Tokuyama H, Wakino S, Itoh H. (2018) High Basolateral Glucose Increases Sodium-Glucose Cotransporter 2 and Reduces Sirtuin-1 in Renal Tubules through Glucose Transporter-2 Detection. Sci Rep, 8: 6791.
21. Komoroski B, Vachharajani N, Boulton D, Kornhauser D, Geraldes M, Li L, Pfister M. (2009) Dapagliflozin, a novel SGLT2 inhibitor, induces dose-dependent glucosuria in healthy subjects. Clin Pharmacol Ther, 85: 520-526.

22. Cefalo CMA, Cinti F, Moffa S, Impronta F, Sorice GP, Mezza T, Pontecorvi A, Giaccari A. (2019) Sotagliflozin, the first dual SGLT inhibitor: current outlook and perspectives. Cardiovasc Diabetol, 18: 20.
23. Rosenstock J, Cefalu WT, Lapuerta P, Zambrowicz B, Ogbaa I, Banks P, Sands A. (2015) Greater dose-ranging effects on A1C levels than on glucosuria with LX4211, a dual inhibitor of SGLT1 and SGLT2, in patients with type 2 diabetes on metformin monotherapy. Diabetes Care, 38: 431-438.
24. Trico D, Baldi S, Tulipani A, Frascerra S, Macedo MP, Mari A, Ferrannini E, Natali A. (2015) Mechanisms through which a small protein and lipid preload improves glucose tolerance. Diabetologia, 58: 2503-2512.
25. McGuire DK, Shih WJ, Cosentino F, Charbonnel B, Cherney DZI, Dagogo-Jack S, Pratley R, Greenberg M, Wang S, Huyck S, Gantz I, Terra SG, Masiukiewicz U, Cannon CP. (2021) Association of SGLT2 Inhibitors With Cardiovascular and Kidney Outcomes in Patients With Type 2 Diabetes: A Meta-analysis. JAMA Cardiol, 6: 148-158.
26. McMurray JJV, Solomon SD, Inzucchi SE, Kober L, Kosiborod MN, Martinez FA, Ponikowski P, Sabatine MS, Anand IS, Belohlavek J, Bohm M, Chiang CE, Chopra VK, de Boer RA, Desai AS, Diez M, Drozdz J, Dukat A, Ge J, Howlett JG, Katova T, Kitakaze M, Ljungman CEA, Merkely B, Nicolau JC, O'Meara E, Petrie MC, Vinh PN, Schou M, Tereshchenko S, Verma S, Held C, DeMets DL, Docherty KF, Jhund PS, Bengtsson O, Sjostrand M, Langkilde AM, Committees D-HT, Investigators. (2019) Dapagliflozin in Patients with Heart Failure and Reduced Ejection Fraction. N Engl J Med, 381: 1995-2008.
27. Packer M, Anker SD, Butler J, Filippatos G, Pocock SJ, Carson P, Januzzi J, Verma S, Tsutsui H, Brueckmann M, Jamal W, Kimura K, Schnee J, Zeller C, Cotton D, Bocchi E, Bohm M, Choi DJ, Chopra V, Chuquiure E, Giannetti N, Janssens S, Zhang J, Gonzalez Juanatey JR, Kaul S, Brunner-La Rocca HP, Merkely B, Nicholls SJ, Perrone S, Pina I, Ponikowski P, Sattar N, Senni M, Seronde MF, Spinar J, Squire I, Taddei S, Wanner C, Zannad F, Investigators EM-RT. (2020) Cardiovascular and Renal Outcomes with Empagliflozin in Heart Failure. N Engl J Med, 383:1413-1424.

28. Bhatt DL, Szarek M, Steg PG, Cannon CP, Leiter LA, McGuire DK, Lewis JB, Riddle MC, Voors AA, Metra M, Lund LH, Komajda M, Testani JM, Wilcox CS, Ponikowski P, Lopes RD, Verma S, Lapuerta P, Pitt B, Investigators S-WT. (2021) Sotagliflozin in Patients with Diabetes and Recent Worsening Heart Failure. N Engl J Med, 384: 117-128.

29. Anker SD, Butler J, Filippatos G, Ferreira JP, Bocchi E, Bohm M, Brunner-La Rocca HP, Choi DJ, Chopra V, Chuquiure-Valenzuela E, Giannetti N, Gomez-Mesa JE, Janssens S, Januzzi JL, Gonzalez-Juanatey JR, Merkely B, Nicholls SJ, Perrone SV, Pina IL, Ponikowski P, Senni M, Sim D, Spinar J, Squire I, Taddei S, Tsutsui H, Verma S, Vinereanu D, Zhang J, Carson P, Lam CSP, Marx N, Zeller C, Sattar N, Jamal W, Schnaidt S, Schnee JM, Brueckmann M, Pocock SJ, Zannad F, Packer M, Investigators EM-PT. (2021) Empagliflozin in Heart Failure with a Preserved Ejection Fraction. N Engl J Med, 385:1451-1461.

30. Solomon SD, McMurray JJV, Claggett B, de Boer RA, DeMets D, Hernandez AF, Inzucchi SE, Kosiborod MN, Lam CSP, Martinez F, Shah SJ, Desai AS, Jhund PS, Belohlavek J, Chiang CE, Borleffs CJW, Comin-Colet J, Dobreanu D, Drozdz J, Fang JC, Alcocer-Gamba MA, Al Habeeb W, Han Y, Cabrera Honorio JW, Janssens SP, Katova T, Kitakaze M, Merkely B, O'Meara E, Saraiva JFK, Tereshchenko SN, Thierer J, Vaduganathan M, Vardeny O, Verma S, Pham VN, Wilderang U, Zaozerska N, Bachus E, Lindholm D, Petersson M, Langkilde AM, Committees DT, Investigators. (2022) Dapagliflozin in Heart Failure with Mildly Reduced or Preserved Ejection Fraction. N Engl J Med, 387: 1089-1098.

31. Authors/Task Force M, McDonagh TA, Metra M, Adamo M, Gardner RS, Baumbach A, Bohm M, Burri H, Butler J, Celutkiene J, Chioncel O, Cleland JGF, Coats AJS, Crespo-Leiro MG, Farmakis D, Gilard M, Heymans S, Hoes AW, Jaarsma T, Jankowska EA, Lainscak M, Lam CSP, Lyon AR, McMurray JJV, Mebazaa A, Mindham R, Muneretto C, Francesco Piepoli M, Price S, Rosano GMC, Ruschitzka F, Kathrine Skibelund A, Group ESCSD. (2022) 2021 ESC Guidelines for the diagnosis and treatment of acute and chronic heart failure: Developed by the Task Force for the diagnosis and treatment of acute and chronic heart failure of the European Society of Cardiology (ESC). With the

special contribution of the Heart Failure Association (HFA) of the ESC. Eur J Heart Fail, 24: 4-131.

32. von Lewinski D, Gasser R, Rainer PP, Huber MS, Wilhelm B, Roessl U, Haas T, Wasler A, Grimm M, Bisping E, Pieske B. (2010) Functional effects of glucose transporters in human ventricular myocardium. Eur J Heart Fail, 12: 106-113.
33. Packer M. (2021) Critical examination of mechanisms underlying the reduction in heart failure events with SGLT2 inhibitors: identification of a molecular link between their actions to stimulate erythrocytosis and to alleviate cellular stress. Cardiovasc Res, 117: 74-84.
34. Cowie MR, Fisher M. (2020) SGLT2 inhibitors: mechanisms of cardiovascular benefit beyond glycaemic control. Nat Rev Cardiol, 17: 761-772.
35. Tamargo J. (2019) Sodium-glucose Cotransporter 2 Inhibitors in Heart Failure: Potential Mechanisms of Action, Adverse Effects and Future Developments. Eur Cardiol, 14: 23-32.
36. Fathi A, Vickneson K, Singh JS. (2021) SGLT2-inhibitors; more than just glycosuria and diuresis. Heart Fail Rev, 26: 623-642.
37. Ferrannini E, Mark M, Mayoux E. (2016) CV Protection in the EMPA-REG OUTCOME Trial: A "Thrifty Substrate" Hypothesis. Diabetes Care, 39: 1108-1114.
38. Bertero E, Prates Roma L, Ameri P, Maack C. (2018) Cardiac effects of SGLT2 inhibitors: the sodium hypothesis. Cardiovasc Res, 114: 12-18.
39. Vallon V, Verma S. (2021) Effects of SGLT2 Inhibitors on Kidney and Cardiovascular Function. Annu Rev Physiol, 83: 503-528.
40. Garcia-Ropero A, Vargas-Delgado AP, Santos-Gallego CG, Badimon JJ. (2019) Inhibition of Sodium Glucose Cotransporters Improves Cardiac Performance. Int J Mol Sci, 20: 3289.
41. Sayour AA, Celeng C, Olah A, Ruppert M, Merkely B, Radovits T. (2021) Sodium-glucose cotransporter 2 inhibitors reduce myocardial infarct size in preclinical animal models of myocardial ischaemia-reperfusion injury: a meta-analysis. Diabetologia, 64: 737-748.

42. Bjornstad P, Greasley PJ, Wheeler DC, Chertow GM, Langkilde AM, Heerspink HJL, van Raalte DH. (2021) The potential roles of osmotic and non-osmotic sodium handling in mediating effects of SGLT2 inhibitors on heart failure. J Card Fail, 27: 1447-1455.
43. Zannad F, Ferreira JP, Pocock SJ, Anker SD, Butler J, Filippatos G, Brueckmann M, Ofstad AP, Pfarr E, Jamal W, Packer M. (2020) SGLT2 inhibitors in patients with heart failure with reduced ejection fraction: a meta-analysis of the EMPEROR-Reduced and DAPA-HF trials. Lancet, 396: 819-829.
44. Nassif ME, Windsor SL, Tang F, Khariton Y, Husain M, Inzucchi SE, McGuire DK, Pitt B, Scirica BM, Austin B, Drazner MH, Fong MW, Givertz MM, Gordon RA, Jermyn R, Katz SD, Lamba S, Lanfear DE, LaRue SJ, Lindenfeld J, Malone M, Margulies K, Mentz RJ, Mutharasan RK, Pursley M, Umpierrez G, Kosiborod M. (2019) Dapagliflozin Effects on Biomarkers, Symptoms, and Functional Status in Patients With Heart Failure With Reduced Ejection Fraction: The DEFINE-HF Trial. Circulation, 140: 1463-1476.
45. Packer M, Anker SD, Butler J, Filippatos G, Ferreira JP, Pocock SJ, Sattar N, Brueckmann M, Jamal W, Cotton D, Iwata T, Zannad F, Committees EM-RT, Investigators. (2021) Empagliflozin in Patients With Heart Failure, Reduced Ejection Fraction, and Volume Overload: EMPEROR-Reduced Trial. J Am Coll Cardiol, 77: 1381-1392.
46. Zhou L, Cryan EV, D'Andrea MR, Belkowski S, Conway BR, Demarest KT. (2003) Human cardiomyocytes express high level of Na+/glucose cotransporter 1 (SGLT1). J Cell Biochem, 90: 339-346.
47. Chen J, Williams S, Ho S, Loraine H, Hagan D, Whaley JM, Feder JN. (2010) Quantitative PCR tissue expression profiling of the human SGLT2 gene and related family members. Diabetes Ther, 1: 57-92.
48. Van Steenbergen A, Balteau M, Ginion A, Ferte L, Battault S, Ravenstein CM, Balligand JL, Daskalopoulos EP, Gilon P, Despa F, Despa S, Vanoverschelde JL, Horman S, Koepsell H, Berry G, Hue L, Bertrand L, Beauloye C. (2017) Sodium-myoinositol cotransporter-1, SMIT1, mediates the production of

reactive oxygen species induced by hyperglycemia in the heart. Sci Rep, 7: 41166.

49. Di Franco A, Cantini G, Tani A, Coppini R, Zecchi-Orlandini S, Raimondi L, Luconi M, Mannucci E. (2017) Sodium-dependent glucose transporters (SGLT) in human ischemic heart: A new potential pharmacological target. Int J Cardiol, 243: 86-90.

50. Baartscheer A, Schumacher CA, Wust RC, Fiolet JW, Stienen GJ, Coronel R, Zuurbier CJ. (2017) Empagliflozin decreases myocardial cytoplasmic Na(+) through inhibition of the cardiac Na(+)/H(+) exchanger in rats and rabbits. Diabetologia, 60: 568-573.

51. Uthman L, Baartscheer A, Bleijlevens B, Schumacher CA, Fiolet JWT, Koeman A, Jancev M, Hollmann MW, Weber NC, Coronel R, Zuurbier CJ. (2018) Class effects of SGLT2 inhibitors in mouse cardiomyocytes and hearts: inhibition of Na(+)/H(+) exchanger, lowering of cytosolic Na(+) and vasodilation. Diabetologia, 61: 722-726.

52. Zuurbier CJ, Baartscheer A, Schumacher CA, Fiolet JWT, Coronel R. (2021) SGLT2 inhibitor empagliflozin inhibits the cardiac Na+/H+ exchanger 1: persistent inhibition under various experimental conditions. Cardiovasc Res, 117: 2699–2701.

53. Uthman L, Nederlof R, Eerbeek O, Baartscheer A, Schumacher C, Buchholtz N, Hollmann MW, Coronel R, Weber NC, Zuurbier CJ. (2019) Delayed ischaemic contracture onset by empagliflozin associates with NHE1 inhibition and is dependent on insulin in isolated mouse hearts. Cardiovasc Res, 115: 1533-1545.

54. Chung YJ, Park KC, Tokar S, Eykyn TR, Fuller W, Pavlovic D, Swietach P, Shattock MJ. (2020) Off-target effects of SGLT2 blockers: empagliflozin does not inhibit Na+/H+ exchanger-1 or lower [Na+]i in the heart. Cardiovasc Res, 117: 2699-2701.

55. Philippaert K, Kalyaanamoorthy S, Fatehi M, Long W, Soni S, Byrne NJ, Barr A, Singh J, Wong J, Palechuk T, Schneider C, Darwesh AM, Maayah ZH, Seubert JM, Barakat K, Dyck JRB, Light PE. (2021) Cardiac Late Sodium Channel Current Is a Molecular Target for the Sodium/Glucose Cotransporter 2 Inhibitor Empagliflozin. Circulation, 143: 2188-2204.

56. Li X, Lu Q, Qiu Y, do Carmo JM, Wang Z, da Silva AA, Mouton A, Omoto ACM, Hall ME, Li J, Hall JE. (2021) Direct Cardiac Actions of the Sodium Glucose Co-Transporter 2 Inhibitor Empagliflozin Improve Myocardial Oxidative Phosphorylation and Attenuate Pressure-Overload Heart Failure. J Am Heart Assoc, 10: e018298.
57. Grempler R, Thomas L, Eckhardt M, Himmelsbach F, Sauer A, Sharp DE, Bakker RA, Mark M, Klein T, Eickelmann P. (2012) Empagliflozin, a novel selective sodium glucose cotransporter-2 (SGLT-2) inhibitor: characterisation and comparison with other SGLT-2 inhibitors. Diabetes Obes Metab, 14: 83-90.
58. Banerjee SK, McGaffin KR, Pastor-Soler NM, Ahmad F. (2009) SGLT1 is a novel cardiac glucose transporter that is perturbed in disease states. Cardiovasc Res, 84: 111-118.
59. Martin MG, Turk E, Lostao MP, Kerner C, Wright EM. (1996) Defects in Na+/glucose cotransporter (SGLT1) trafficking and function cause glucose-galactose malabsorption. Nat Genet, 12: 216-220.
60. Seidelmann SB, Feofanova E, Yu B, Franceschini N, Claggett B, Kuokkanen M, Puolijoki H, Ebeling T, Perola M, Salomaa V, Shah A, Coresh J, Selvin E, MacRae CA, Cheng S, Boerwinkle E, Solomon SD. (2018) Genetic Variants in SGLT1, Glucose Tolerance, and Cardiometabolic Risk. J Am Coll Cardiol, 72: 1763-1773.
61. Katzmann JL, Mason AM, Marz W, Kleber ME, Niessner A, Bluher M, Speer T, Laufs U. (2021) Genetic variation in sodium-glucose cotransporter 2 and heart failure. Clin Pharmacol Ther, 110: 149-158.
62. Elfeber K, Stumpel F, Gorboulev V, Mattig S, Deussen A, Kaissling B, Koepsell H. (2004) Na(+)-D-glucose cotransporter in muscle capillaries increases glucose permeability. Biochem Biophys Res Commun, 314: 301-305.
63. Meng L, Uzui H, Guo H, Tada H. (2018) Role of SGLT1 in high glucose level-induced MMP-2 expression in human cardiac fibroblasts. Mol Med Rep, 17: 6887-6892.
64. Sawa Y, Saito M, Ishida N, Ibi M, Matsushita N, Morino Y, Taira E, Hirose M. (2020) Pretreatment with KGA-2727, a selective SGLT1 inhibitor, is protective

against myocardial infarction-induced ventricular remodeling and heart failure in mice. J Pharmacol Sci, 142: 16-25.

65. Kanwal A, Nizami HL, Mallapudi S, Putcha UK, Mohan GK, Banerjee SK. (2016) Inhibition of SGLT1 abrogates preconditioning-induced cardioprotection against ischemia-reperfusion injury. Biochem Biophys Res Commun, 472: 392-398.

66. Banerjee SK, Wang DW, Alzamora R, Huang XN, Pastor-Soler NM, Hallows KR, McGaffin KR, Ahmad F. (2010) SGLT1, a novel cardiac glucose transporter, mediates increased glucose uptake in PRKAG2 cardiomyopathy. J Mol Cell Cardiol, 49: 683-692.

67. Lambert R, Srodulski S, Peng X, Margulies KB, Despa F, Despa S. (2015) Intracellular Na+ Concentration ([Na+]i) Is Elevated in Diabetic Hearts Due to Enhanced Na+-Glucose Cotransport. J Am Heart Assoc, 4: e002183.

68. Li Z, Agrawal V, Ramratnam M, Sharma RK, D'Auria S, Sincoular A, Jakubiak M, Music ML, Kutschke WJ, Huang XN, Gifford L, Ahmad F. (2019) Cardiac sodium-dependent glucose cotransporter 1 is a novel mediator of ischaemia/reperfusion injury. Cardiovasc Res, 115: 1646-1658.

69. Vrhovac I, Balen Eror D, Klessen D, Burger C, Breljak D, Kraus O, Radovic N, Jadrijevic S, Aleksic I, Walles T, Sauvant C, Sabolic I, Koepsell H. (2015) Localizations of Na(+)-D-glucose cotransporters SGLT1 and SGLT2 in human kidney and of SGLT1 in human small intestine, liver, lung, and heart. Pflugers Arch, 467: 1881-1898.

70. Sanchez-Mas J, Saura-Guillen E, Asensio-Lopez MC, Soriano-Filiu A, Carmen Sanchez-Perez M, Hernandez-Martinez AM, Lax A, Pascual-Figal D. (2019) Temporal characterization of cardiac expression of glucose transporters SGLT and GLUT in an experimental model of myocardial infarction. Diabetes Metab, 45: 201-204.

71. Matsushita N, Ishida N, Ibi M, Saito M, Sanbe A, Shimojo H, Suzuki S, Koepsell H, Takeishi Y, Morino Y, Taira E, Sawa Y, Hirose M. (2018) Chronic Pressure Overload Induces Cardiac Hypertrophy and Fibrosis via Increases in SGLT1 and IL-18 Gene Expression in Mice. Int Heart J, 59: 1123-1133.

72. Ye Y, Bajaj M, Yang HC, Perez-Polo JR, Birnbaum Y. (2017) SGLT-2 Inhibition with Dapagliflozin Reduces the Activation of the Nlrp3/ASC Inflammasome and Attenuates the Development of Diabetic Cardiomyopathy in Mice with Type 2 Diabetes. Further Augmentation of the Effects with Saxagliptin, a DPP4 Inhibitor. Cardiovasc Drugs Ther, 31: 119-132.
73. Sun Z, Chai Q, Zhang Z, Lu D, Meng Z, Wu W. (2021) Inhibition of SGLT1 protects against glycemic variability-induced cardiac damage and pyroptosis of cardiomyocytes in diabetic mice. Life Sci, 271: 119116.
74. Wu W, Chai Q, Zhang Z. (2021) Glucose fluctuation accelerates cardiac injury of diabetic mice via sodium-dependent glucose cotransporter 1 (SGLT1). Arch Biochem Biophys, 709: 108968.
75. Lin H, Guan L, Meng L, Uzui H, Guo H. (2021) SGLT1 Knockdown Attenuates Cardiac Fibroblast Activation in Diabetic Cardiac Fibrosis. Frontiers in Pharmacology, 12: 700366.
76. Yoshii A, Nagoshi T, Kashiwagi Y, Kimura H, Tanaka Y, Oi Y, Ito K, Yoshino T, Tanaka TD, Yoshimura M. (2019) Cardiac ischemia-reperfusion injury under insulin-resistant conditions: SGLT1 but not SGLT2 plays a compensatory protective role in diet-induced obesity. Cardiovasc Diabetol, 18: 85.
77. Connelly KA, Zhang Y, Desjardins JF, Thai K, Gilbert RE. (2018) Dual inhibition of sodium-glucose linked cotransporters 1 and 2 exacerbates cardiac dysfunction following experimental myocardial infarction. Cardiovasc Diabetol, 17: 99.
78. Kashiwagi Y, Nagoshi T, Yoshino T, Tanaka TD, Ito K, Harada T, Takahashi H, Ikegami M, Anzawa R, Yoshimura M. (2015) Expression of SGLT1 in human hearts and impairment of cardiac glucose uptake by phlorizin during ischemia-reperfusion injury in mice. PLoS One, 10: e0130605.
79. Ramratnam M, Sharma RK, D'Auria S, Lee SJ, Wang D, Huang XY, Ahmad F. (2014) Transgenic knockdown of cardiac sodium/glucose cotransporter 1 (SGLT1) attenuates PRKAG2 cardiomyopathy, whereas transgenic overexpression of cardiac SGLT1 causes pathologic hypertrophy and dysfunction in mice. J Am Heart Assoc, 3: e000899.

80. Sala-Rabanal M, Hirayama BA, Ghezzi C, Liu J, Huang SC, Kepe V, Koepsell H, Yu A, Powell DR, Thorens B, Wright EM, Barrio JR. (2016) Revisiting the physiological roles of SGLTs and GLUTs using positron emission tomography in mice. J Physiol, 594: 4425-4438.
81. Ferte L, Marino A, Battault S, Bultot L, Van Steenbergen A, Bol A, Cumps J, Ginion A, Koepsell H, Dumoutier L, Hue L, Horman S, Bertrand L, Beauloye C. (2021) New insight in understanding the contribution of SGLT1 in cardiac glucose uptake: evidence for a truncated form in mice and humans. Am J Physiol Heart Circ Physiol, 320: H838-H853.
82. Balteau M, Tajeddine N, de Meester C, Ginion A, Des Rosiers C, Brady NR, Sommereyns C, Horman S, Vanoverschelde JL, Gailly P, Hue L, Bertrand L, Beauloye C. (2011) NADPH oxidase activation by hyperglycaemia in cardiomyocytes is independent of glucose metabolism but requires SGLT1. Cardiovasc Res, 92: 237-246.
83. Pitt B, Steg G, Leiter LA, Bhatt DL. (2021) The Role of Combined SGLT1/SGLT2 Inhibition in Reducing the Incidence of Stroke and Myocardial Infarction in Patients with Type 2 Diabetes Mellitus. Cardiovasc Drugs Ther, 36: 561-567.
84. Simon J, Nemeth E, Nemes A, Husveth-Toth M, Radovits T, Foldes G, Kiss L, Bagyura Z, Skopal J, Merkely B, Gara E. (2019) Circulating Relaxin-1 Level Is a Surrogate Marker of Myocardial Fibrosis in HFrEF. Front Physiol, 10: 690.
85. Palvolgyi A, Simpson J, Bodnar I, Biro J, Palkovits M, Radovits T, Skehel P, Antoni FA. (2018) Auto-inhibition of adenylyl cyclase 9 (AC9) by an isoform-specific motif in the carboxyl-terminal region. Cell Signal, 51: 266-275.
86. Vanderheyden M, Mullens W, Delrue L, Goethals M, de Bruyne B, Wijns W, Geelen P, Verstreken S, Wellens F, Bartunek J. (2008) Myocardial gene expression in heart failure patients treated with cardiac resynchronization therapy responders versus nonresponders. J Am Coll Cardiol, 51: 129-136.
87. Reiman M, Laan M, Rull K, Sober S. (2017) Effects of RNA integrity on transcript quantification by total RNA sequencing of clinically collected human placental samples. FASEB J, 31: 3298-3308.

88. Gundewar S, Calvert JW, Jha S, Toedt-Pingel I, Ji SY, Nunez D, Ramachandran A, Anaya-Cisneros M, Tian R, Lefer DJ. (2009) Activation of AMP-activated protein kinase by metformin improves left ventricular function and survival in heart failure. Circ Res, 104: 403-411.
89. Zhuo XZ, Wu Y, Ni YJ, Liu JH, Gong M, Wang XH, Wei F, Wang TZ, Yuan Z, Ma AQ, Song P. (2013) Isoproterenol instigates cardiomyocyte apoptosis and heart failure via AMPK inactivation-mediated endoplasmic reticulum stress. Apoptosis, 18: 800-810.
90. Sasaki H, Asanuma H, Fujita M, Takahama H, Wakeno M, Ito S, Ogai A, Asakura M, Kim J, Minamino T, Takashima S, Sanada S, Sugimachi M, Komamura K, Mochizuki N, Kitakaze M. (2009) Metformin prevents progression of heart failure in dogs: role of AMP-activated protein kinase. Circulation, 119: 2568-2577.
91. Gonzalez A, Ravassa S, Loperena I, Lopez B, Beaumont J, Querejeta R, Larman M, Diez J. (2007) Association of depressed cardiac gp130-mediated antiapoptotic pathways with stimulated cardiomyocyte apoptosis in hypertensive patients with heart failure. J Hypertens, 25: 2148-2157.
92. Schnelle M, Sawyer I, Anilkumar N, Mohamed BA, Richards DA, Toischer K, Zhang M, Catibog N, Sawyer G, Mongue-Din H, Schroder K, Hasenfuss G, Shah AM. (2021) NADPH oxidase-4 promotes eccentric cardiac hypertrophy in response to volume overload. Cardiovasc Res, 117: 178-187.
93. Li XM, Ma YT, Yang YN, Liu F, Chen BD, Han W, Zhang JF, Gao XM. (2009) Downregulation of survival signalling pathways and increased apoptosis in the transition of pressure overload-induced cardiac hypertrophy to heart failure. Clin Exp Pharmacol Physiol, 36: 1054-1061.
94. Kehat I, Davis J, Tiburcy M, Accornero F, Saba-El-Leil MK, Maillet M, York AJ, Lorenz JN, Zimmermann WH, Meloche S, Molkentin JD. (2011) Extracellular signal-regulated kinases 1 and 2 regulate the balance between eccentric and concentric cardiac growth. Circ Res, 108: 176-183.
95. Han HJ, Park SH, Lee YJ. (2004) Signaling cascade of ANG II-induced inhibition of alpha-MG uptake in renal proximal tubule cells. Am J Physiol Renal Physiol, 286: F634-642.

96. Jae Han H, Yeong Park J, Jung Lee Y, Taub M. (2004) Epidermal growth factor inhibits 14C-alpha-methyl-D-glucopyranoside uptake in renal proximal tubule cells: involvement of PLC/PKC, p44/42 MAPK, and cPLA2. J Cell Physiol, 199: 206-216.

97. Maack C, Cortassa S, Aon MA, Ganesan AN, Liu T, O'Rourke B. (2006) Elevated cytosolic Na+ decreases mitochondrial Ca2+ uptake during excitation-contraction coupling and impairs energetic adaptation in cardiac myocytes. Circ Res, 99: 172-182.

98. Kondo H, Akoumianakis I, Badi I, Akawi N, Kotanidis CP, Polkinghorne M, Stadiotti I, Sommariva E, Antonopoulos AS, Carena MC, Oikonomou EK, Reus EM, Sayeed R, Krasopoulos G, Srivastava V, Farid S, Chuaiphichai S, Shirodaria C, Channon KM, Casadei B, Antoniades C. (2021) Effects of canagliflozin on human myocardial redox signalling: clinical implications. Eur Heart J, 42: 4947-4960.

99. Tager T, Frankenstein L, Atar D, Agewall S, Frey N, Grundtvig M, Clark AL, Cleland JGF, Frohlich H. (2021) Influence of receptor selectivity on benefits from SGLT2 inhibitors in patients with heart failure: a systematic review and head-to-head comparative efficacy network meta-analysis. Clin Res Cardiol, 111:428-439.

9. Bibliography of the candidate's publications

9.1. Publications directly related to the present thesis

Sayour AA, Olah A, Ruppert M, Barta BA, Horvath EM, Benke K, Polos M, Hartyanszky I, Merkely B, Radovits T. (2020) Characterization of left ventricular myocardial sodium-glucose cotransporter 1 expression in patients with end-stage heart failure. Cardiovasc Diabetol, 19: 159. (SJR D1, IF=9.951)

Sayour AA, Ruppert M, Olah A, Benke K, Barta BA, Zsary E, Ke H, Horvath EM, Merkely B, Radovits T. (2021) Left Ventricular SGLT1 Protein Expression Correlates with the Extent of Myocardial Nitro-Oxidative Stress in Rats with Pressure and Volume Overload-Induced Heart Failure. Antioxidants (Basel), 10: 1190. (SJR Q1, IF=7.675)

Sayour AA, Ruppert M, Olah A, Benke K, Barta BA, Zsary E, Merkely B, Radovits T. (2021) Effects of SGLT2 Inhibitors beyond Glycemic Control-Focus on Myocardial SGLT1. Int J Mol Sci, 22: 9852. (SJR D1, IF=6.208)

9.2. Publications not directly related to the present thesis

9.2.1. Publications in international peer–reviewed journals

Ding Q, Loganathan S, Zhou P, **Sayour AA**, Brlecic P, Radovits T, Domain R, Korkmaz B, Karck M, Szabo G, Korkmaz-Icoz S. (2023) Alpha-1-Antitrypsin Protects Vascular Grafts of Brain-Dead Rats Against Ischemia/Reperfusion Injury. J Surg Res, 283: 953-964.

Sayour AA, Tokodi M, Celeng C, Takx RAP, Fabian A, Lakatos BK, Friebel R, Surkova E, Merkely B, Kovacs A. (2023) Association of Right Ventricular Functional Parameters With Adverse Cardiopulmonary Outcomes: A Meta-analysis. J Am Soc Echocardiogr, doi:10.1016/j.echo.2023.01.018.

Korkmaz-Icoz S, Sistori G, Loganathan S, **Sayour AA**, Brlecic P, Radovits T, Brune M, Karck M, Szabo G. (2022) Bone Marrow Culture-Derived Conditioned Medium Recovers Endothelial Function of Vascular Grafts following In Vitro Ischemia/Reperfusion Injury in Diabetic Rats. Stem Cells Int, 2022: 7019088.

Ruppert M, Barta BA, Korkmaz-Icoz S, Loganathan S, Olah A, **Sayour AA**, Benke K, Nagy D, Balint T, Karck M, Schilling O, Merkely B, Radovits T, Szabo G. (2022) Sex similarities and differences in the reverse and anti-remodeling effect of pressure unloading therapy in a rat model of aortic banding and debanding. Am J Physiol Heart Circ Physiol, 323: H204-H222.

Kugler S, Onodi Z, Ruppert M, **Sayour AA**, Olah A, Benke K, Ferdinandy P, Merkely B, Radovits T, Varga ZV. (2022) Inflammasome activation in end-stage heart failure-associated atrial fibrillation. ESC Heart Fail, 9: 2747-2752.

Veres G, Benke K, Stengl R, Bai Y, Stark KA, **Sayour AA**, Radovits T, Loganathan S, Korkmaz-Icoz S, Karck M, Szabo G. (2022) Aspirin Reduces Ischemia-Reperfusion Injury Induced Endothelial Cell Damage of Arterial Grafts in a Rodent Model. Antioxidants (Basel), 11.

Barta BA, Ruppert M, Frohlich KE, Cosenza-Contreras M, Olah A, **Sayour AA**, Kovacs K, Karvaly GB, Biniossek M, Merkely B, Schilling O, Radovits T. (2021) Sex-related differences of early cardiac functional and proteomic alterations in a rat model of myocardial ischemia. J Transl Med, 19: 507.

Korkmaz-Icoz S, Ballikaya B, Soethoff J, Kraft P, **Sayour AA**, Radovits T, Loganathan S, Karck M, Szabo G, Veres G. (2021) Graft Preservation Solution DuraGraft((R)) Alleviates Vascular Dysfunction Following In Vitro Ischemia/Reperfusion Injury in Rats. Pharmaceuticals (Basel), 14.

Tokodi M, Olah A, Fabian A, Lakatos BK, Hizoh I, Ruppert M, **Sayour AA**, Barta BA, Kiss O, Sydo N, Csulak E, Ladanyi Z, Merkely B, Kovacs A, Radovits T. (2022) Novel insights into the athlete's heart: is myocardial work the new champion of systolic function? Eur Heart J Cardiovasc Imaging, 23: 188-197.

Korkmaz-Icoz S, Kocer C, **Sayour AA**, Kraft P, Benker MI, Abulizi S, Georgevici AI, Brlecic P, Radovits T, Loganathan S, Karck M, Szabo G. (2021) The Sodium-Glucose Cotransporter-2 Inhibitor Canagliflozin Alleviates Endothelial Dysfunction Following In Vitro Vascular Ischemia/Reperfusion Injury in Rats. Int J Mol Sci, 22.

Onodi Z, Ruppert M, Kucsera D, **Sayour AA**, Toth VE, Koncsos G, Novak J, Brenner GB, Makkos A, Baranyai T, Giricz Z, Gorbe A, Leszek P, Gyongyosi M, Horvath IG, Schulz R, Merkely B, Ferdinandy P, Radovits T, Varga ZV. (2021) AIM2-driven inflammasome activation in heart failure. Cardiovasc Res, 117: 2639-2651.

Korkmaz-Icoz S, Sun X, Li S, Brlecic P, Loganathan S, Ruppert M, **Sayour AA**, Radovits T, Karck M, Szabo G. (2021) Conditioned Medium from Mesenchymal Stem Cells Alleviates Endothelial Dysfunction of Vascular Grafts Submitted to Ischemia/Reperfusion Injury in 15-Month-Old Rats. Cells, 10.

Torok M, Merkely P, Monori-Kiss A, Horvath EM, Sziva RE, Peterffy B, Josvai A, **Sayour AA**, Olah A, Radovits T, Merkely B, Acs N, Nadasy GL, Varbiro S. (2021) Network analysis of the left anterior descending coronary arteries in swim-trained rats by an in situ video microscopic technique. Biol Sex Differ, 12: 37.

Korkmaz-Icoz S, Akca D, Li S, Loganathan S, Brlecic P, Ruppert M, **Sayour AA**, Simm A, Brune M, Radovits T, Karck M, Szabo G. (2021) Left-ventricular hypertrophy in 18-month-old donor rat hearts was not associated with graft dysfunction in the early phase of reperfusion after cardiac transplantation-gene expression profiling. Geroscience, 43: 1995-2013.

Tokodi M, Lakatos BK, Ruppert M, Fabian A, Olah A, **Sayour AA**, Ladanyi Z, Soos A, Merkely B, Sengupta PP, Radovits T, Kovacs A. (2021) Left Ventricular Pressure-Strain-Volume Loops for the Noninvasive Assessment of Volume Overload-Induced Myocardial Dysfunction. JACC Cardiovasc Imaging, 14: 1868-1871.

Olah A, Barta BA, **Sayour AA**, Ruppert M, Virag-Tulassay E, Novak J, Varga ZV, Ferdinandy P, Merkely B, Radovits T. (2021) Balanced Intense Exercise Training Induces Atrial Oxidative Stress Counterbalanced by the Antioxidant System and Atrial Hypertrophy That Is Not Associated with Pathological Remodeling or Arrhythmogenicity. Antioxidants (Basel), 10.

Lakatos BK, Ruppert M, Tokodi M, Olah A, Braun S, Karime C, Ladanyi Z, **Sayour AA**, Barta BA, Merkely B, Radovits T, Kovacs A. (2021) Myocardial work index: a marker of left ventricular contractility in pressure- or volume overload-induced heart failure. ESC Heart Fail, 8: 2220-2231.

Korkmaz-Icoz S, Zhou P, Guo Y, Loganathan S, Brlecic P, Radovits T, **Sayour AA**, Ruppert M, Veres G, Karck M, Szabo G. (2021) Mesenchymal stem cell-derived conditioned medium protects vascular grafts of brain-dead rats against in vitro ischemia/reperfusion injury. Stem Cell Res Ther, 12: 144.

Sayour AA, Celeng C, Olah A, Ruppert M, Merkely B, Radovits T. (2021) Sodium-glucose cotransporter 2 inhibitors reduce myocardial infarct size in preclinical animal models of myocardial ischaemia-reperfusion injury: a meta-analysis. Diabetologia, 64: 737-748.

Ruppert M, Lakatos BK, Braun S, Tokodi M, Karime C, Olah A, **Sayour AA**, Hizoh I, Barta BA, Merkely B, Kovacs A, Radovits T. (2020) Longitudinal Strain Reflects Ventriculoarterial Coupling Rather Than Mere Contractility in Rat Models of Hemodynamic Overload-Induced Heart Failure. J Am Soc Echocardiogr, 33: 1264-1275 e1264.

Torok M, Horvath EM, Monori-Kiss A, E PA, Gerszi D, Merkely P, **Sayour AA**, C MA, Olah A, Radovits T, Merkely B, Acs N, GL NA, S VA. (2021) Chronic swimming training resulted in more relaxed coronary arterioles in male and enhanced vasoconstrictor ability in female rats. J Sports Med Phys Fitness, 61: 489-496.

Benke K, Nemeth BT, **Sayour AA**, Stark KA, Olah A, Ruppert M, Szabo G, Korkmaz-Icoz S, Horvath EM, Benko R, Hartyanszky I, Szabolcs Z, Merkely B, Radovits T. (2020) Stimulation of soluble guanylate cyclase improves donor organ function in rat heart transplantation. Sci Rep, 10: 5358.

Korkmaz-Icoz S, Li K, Loganathan S, Ding Q, Ruppert M, Radovits T, Brlecic P, **Sayour AA**, Karck M, Szabo G. (2020) Brain-dead donor heart conservation with a preservation solution supplemented by a conditioned medium from mesenchymal stem cells improves graft contractility after transplantation. Am J Transplant, 20: 2847-2856.

Loganathan S, Guo Y, Jiang W, Radovits T, Ruppert M, **Sayour AA**, Brune M, Brlecic P, Gude P, Georgevici AI, Yard B, Karck M, Korkmaz-Icoz S, Szabo G. (2019) N-octanoyl dopamine is superior to dopamine in protecting graft contractile function when administered to the heart transplant recipients from brain-dead donors. Pharmacol Res, 150: 104503.

Olah A, Matyas C, Kellermayer D, Ruppert M, Barta BA, **Sayour AA**, Torok M, Koncsos G, Giricz Z, Ferdinandy P, Merkely B, Radovits T. (2019) Sex Differences in Morphological and Functional Aspects of Exercise-Induced Cardiac Hypertrophy in a Rat Model. Front Physiol, 10: 889.

Ruppert M, Korkmaz-Icoz S, Loganathan S, Jiang W, Olah A, **Sayour AA**, Barta BA, Karime C, Merkely B, Karck M, Radovits T, Szabo G. (2019) Incomplete structural reverse remodeling from late-stage left ventricular hypertrophy impedes the recovery of diastolic but not systolic dysfunction in rats. J Hypertens, 37: 1200-1212.

Sayour AA, Korkmaz-Icoz S, Loganathan S, Ruppert M, Sayour VN, Olah A, Benke K, Brune M, Benko R, Horvath EM, Karck M, Merkely B, Radovits T, Szabo G. (2019) Acute canagliflozin treatment protects against in vivo myocardial ischemia-reperfusion injury in non-diabetic male rats and enhances endothelium-dependent vasorelaxation. J Transl Med, 17: 127.

Ruppert M, Bodi B, Korkmaz-Icoz S, Loganathan S, Jiang W, Lehmann L, Olah A, Barta BA, **Sayour AA**, Merkely B, Karck M, Papp Z, Szabo G, Radovits T. (2019) Myofilament Ca(2+) sensitivity correlates with left ventricular contractility during the progression of pressure overload-induced left ventricular myocardial hypertrophy in rats. J Mol Cell Cardiol, 129: 208-218.

Korkmaz-Icoz S, Li S, Huttner R, Ruppert M, Radovits T, Loganathan S, **Sayour AA**, Brlecic P, Lasitschka F, Karck M, Szabo G. (2019) Hypothermic perfusion of donor heart with a preservation solution supplemented by mesenchymal stem cells. J Heart Lung Transplant, 38: 315-326.

Olah A, Kovacs A, Lux A, Tokodi M, Braun S, Lakatos BK, Matyas C, Kellermayer D, Ruppert M, **Sayour AA**, Barta BA, Merkely B, Radovits T. (2019) Characterization of the dynamic changes in left ventricular morphology and function induced by exercise training and detraining. Int J Cardiol, 277: 178-185.

Korkmaz-Icoz S, Li S, Loganathan S, Radovits T, Ruppert M, Brlecic P, **Sayour AA**, Veres G, Fleming T, Brune M, Most P, Karck M, Szabo G. (2018) Impairment of the Akt pathway in transplanted Type 1 diabetic hearts is associated with post-transplant graft injury. Interact Cardiovasc Thorac Surg, 27: 884-894.

Ruppert M, Korkmaz-Icoz S, Loganathan S, Jiang W, Lehmann L, Olah A, **Sayour AA**, Barta BA, Merkely B, Karck M, Radovits T, Szabo G. (2018) Pressure-volume analysis reveals characteristic sex-related differences in cardiac function in a rat model of aortic banding-induced myocardial hypertrophy. Am J Physiol Heart Circ Physiol, 315: H502-H511.

Veres G, Hagenhoff M, Schmidt H, Radovits T, Loganathan S, Bai Y, Korkmaz-Icoz S, Brlecic P, **Sayour AA**, Karck M, Szabo G. (2018) Targeting Phosphodiesterase-5 by Vardenafil Improves Vascular Graft Function. Eur J Vasc Endovasc Surg, 56: 256-263.

Benke K, Barabas JI, Daroczi L, **Sayour AA**, Szilveszter B, Polos M, Lux A, Szekely A, Radovits T, Hartyanszky I, Merkely B, Szabolcs Z. (2017) Routine aortic valve replacement followed by a myriad of complications: role of 3D printing in a difficult cardiac surgical case. J Thorac Dis, 9: E1021-E1024.

Benke K, Matyas C, **Sayour AA**, Olah A, Nemeth BT, Ruppert M, Szabo G, Kokeny G, Horvath EM, Hartyanszky I, Szabolcs Z, Merkely B, Radovits T. (2017) Pharmacological preconditioning with gemfibrozil preserves cardiac function after heart transplantation. Sci Rep, 7: 14232.

Benke K, Agg B, Polos M, **Sayour AA**, Radovits T, Bartha E, Nagy P, Rakoczi B, Koller A, Szokolai V, Hedberg J, Merkely B, Nagy ZB, Szabolcs Z. (2017) The effects of acute and elective cardiac surgery on the anxiety traits of patients with Marfan syndrome. BMC Psychiatry, 17: 253.

Benke K*, **Sayour AA***, Matyas C, Agg B, Nemeth BT, Olah A, Ruppert M, Hartyanszky I, Szabolcs Z, Radovits T, Merkely B, Szabo G. (2017) Heterotopic Abdominal Rat Heart Transplantation as a Model to Investigate Volume Dependency of Myocardial Remodeling. Transplantation, 101: 498-505. *Contributed equally.

Olah A, Kellermayer D, Matyas C, Nemeth BT, Lux A, Szabo L, Torok M, Ruppert M, Meltzer A, **Sayour AA**, Benke K, Hartyanszky I, Merkely B, Radovits T. (2017) Complete Reversion of Cardiac Functional Adaptation Induced by Exercise Training. Med Sci Sports Exerc, 49: 420-429.

Olah A, Nemeth BT, Matyas C, Hidi L, Lux A, Ruppert M, Kellermayer D, **Sayour AA**, Szabo L, Torok M, Meltzer A, Geller L, Merkely B, Radovits T. (2016) Physiological and pathological left ventricular hypertrophy of comparable degree is associated with characteristic differences of in vivo hemodynamics. Am J Physiol Heart Circ Physiol, 310: H587-597.

9.2.2. Publications in Hungarian peer–reviewed journals

Barczi G, Merkely B, Olah A, Papp S, **Sayour AA**, Szigyarto I, Zoka A, Becker D. (2023) Myocardialis izomhíd: a tüneteket befolyásoló morfológiai faktorok vizsgálata. Orv Hetil, 164: 563-570.

Sayour AA, Ruppert M, Olah A, Benke K, Benko R, Horvath EM, Korkmaz-Icoz S, Loganathan S, Karck M, Merkely B, Szabo G, Radovits T. (2020) Az akut canagliflozin kezelés kivédi a miokardiális iszkémia-reperfúziós károsodást patkánymodellen. Cardiol Hung, 50: 417-427.

Ruppert M, Bodi B, Nagy D, Korkmaz-Icoz S, Loganathan S, Olah A, Barta BA, **Sayour AA**, Benke K, Karck M, Merkely B, Szabo G, Radovits T. (2019) A miofilamentáris rendszer Ca2+-érzékenysége korrellál a bal kamrai kontraktilitással a fokozott nyomásterhelés által előidézett patológiás szívizom-hipertrófia patkánymodelljében. Cardiol Hung, 49: 88-99.

Ruppert M, Barta BA, Korkmaz-Icoz S, Li S, Olah A, Matyas C, Nemeth BT, Benke K, **Sayour AA**, Karck M, Merkely B, Szabo G, Radovits T. (2018) A hipertrófiás myocardium reverz elektromos remodellációjának vizsgálata patkánymodellben. Cardiol Hung, 48: 118-128.

Olah A*, **Sayour AA***, Nemeth BT, Matyas C, Hidi L, Lux A, Ruppert M, Kellermayer D, Szabo L, Torok M, Meltzer A, Geller L, Merkely B, Radovits T. (2018) A hasonló fokú fiziológiás és patológiás balkamra-hipertrófia különböző in vivo hemodinamikai következményekhez vezet. Cardiol Hung, 48: 20-30. *Contributed equally.

Matyas C*, **Sayour AA***, Korkmaz-Icoz S, Olah A, Nemeth BT, Pali S, Hirschberg K, Zubarevich A, Gwanmesia PN, Li S, Loganathan S, Barnucz E, Merkely B, Szabo G, Radovits T. (2017) Az 1-es és 2-es típusú diabéteszes kardiális diszfunkció hátterében álló eltérő miokardiális szövettani és molekuláris jellegzetességek. Cardiol Hung 47: 102-111. *Contributed equally.

Benke K*, **Sayour AA***, Agg B, Radovits T, Szilveszter B, Odler B, Nemeth BT, Polos M, Olah A, Matyas C, Ruppert M, Hartyanszky I, Maurovich-Horvat P, Merkely B, Szabolcs Z. (2016) Génpolimorfizmusok, mint rizikófaktorok a Marfan-szindróma kardiovaszkuláris manifesztációinak előrejelzésében. Cardiol Hung, 46: 76-81. *Contributed equally.

10. Acknowledgements

I am indebted to several people for their continuous support, without whom the present thesis could not have been written.

First, I would like to thank my scientific supervisor Prof. Dr. Tamás Radovits for his continued support ever since I joined his Team as a research student in 2014. I appreciate that I had a unique opportunity to learn scientific thinking, operative models, and molecular measurements from him. All these skills were prerequisite for my thesis and will accompany me throughout my scientific career. Hereby, I express my sincere gratitude to Prof. Dr. Béla Merkely, who provided the background to my research, continuously supported me all the way, and always lead me to the right direction.

I thank all my co-authors, especially Dr. Attila Oláh and Dr. Mihály Ruppert, for their invaluable support not only in the scientific field, but also in clinical practice. I am grateful to Dr. Kálmán Benke, who saw the potential in me from the very beginning and assisted me to start my scientific career. I also thank all former and current members of the research laboratory, especially Henriett Biró, Benjámin Prokaj, and Edina Urbán.

I am grateful to have been given the chance to join the experimental research laboratory of the Department of Cardiac Surgery, University Hospital Heidelberg, Heidelberg, Germany, with the lead of Prof. Dr. Gábor Szabó and Dr. Sevil Korkmaz-Icöz. I believe I have gained invaluable experience during my one-year visit.

Last but not least, I am indebted to my whole family for incessantly assisting me in fulfilling my dreams and continuously helping me throughout my career. I would like to express my sincere gratitude to my wife, Dr. Krisztina Mekler, for the infinite motivation she has given me throughout the years, even in the most difficult situations. Without her continuous support, this thesis would not have been written. At the time of the writing of this thesis, we are eagerly expecting our first child, Emma, to whom I dedicate this work.